


Recent developments in chemistry, coordination, structure and biological aspects of 1-(acyl/aroyl)-3-(substituted) thioureas

Aamer Saeed¹  · Rabia Qamar¹ · Tanzeela Abdul Fattah¹ · Ulrich Flörke² · Mauricio F. Erben³

Received: 16 September 2016 / Accepted: 8 November 2016
© Springer Science+Business Media Dordrecht 2016

Abstract 1-(Acyl/aroyl)-3-(substituted)thioureas are privileged architectures that have received remarkable attention of researchers in view of their variable topological aspects, binding modes and broad spectrum promising pharmacological properties. Reactivity of acyl thiourea derivatives has presented various organic transformations into other demanding scaffolds and this is an attractive strategy for synthetic chemists to access heterocyclic cores. Multiple binding sites make them flexible ligands for complexation with transition metals thus occupying a distinct position in coordination chemistry. 1-(Acyl/aroyl)-3-(substituted)thioureas have also emerged as attractive candidates in various fields such as ion sensors, corrosion inhibitors, molecular electronics, in metal extraction and in pharmaceuticals. The medicinal chemistry of this organo-sulfur framework and the derived metal complexes has witnessed fantastic progress in the current era. In continuation of our efforts to compile data on the structural aspects and numerous applications of 1-(acyl/aroyl)-3-(substituted)thiourea analogs, continuous advances have prompted us to present an overview of the last 2 years literature on this exciting family of compounds through this review article.

Keywords Acyl thiourea · Ion sensors · Electronics · Corrosion · Medicinal

✉ Aamer Saeed
aamersaeed@yahoo.com

¹ Department of Chemistry, Quaid-i-Azam University, Islamabad 45320, Pakistan

² Department Chemie, Fakultät für Naturwissenschaften, Universität Paderborn, Warburgerstrasse 100, 33098 Paderborn, Germany

³ CEQUINOR (UNLP, CONICET-CCT La Plata), Departamento de Química, Facultad de Ciencias Exactas, Universidad Nacional de La Plata, C.C. 962 (1900), La Plata, Argentine Republic

Introduction

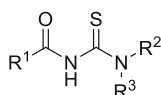
The chemistry of acyl thioureas is enjoying a prestigious status as evidenced by the fact that this molecular architecture has become the center of attraction to the scientific community for many years. The general structure of 1-(acyl/aryl)-3-(mono or di-alkyl/aryl)thiourea is shown in Scheme 1.

The straightforward synthetic route and excellent properties are the key features which constantly engage many researchers in efforts to explore more and more such multipurpose thio compounds [1–3]. They have been the subject of extensive study in coordination chemistry [4], and are also known to play a promising role in the fields of material sciences, molecular electronics, molecular recognition, agriculture, biological activities and pharmaceuticals. The presence of both soft and hard donors within the same molecular framework facilitates title compounds to be applied as ion sensors and transition metal extractors [5, 6].

Many reported examples have demonstrated the varied biological activities of thioureas, such as antitumor [7], antiviral [8], antimicrobial [9], antiparasitic [10], insecticidal [11], herbicidal [12], pesticidal and fungicidal properties [13, 14]. The 1*H*-benzimidazol thiourea derivatives evolved as promising anti-HIV and antibacterial agents [15, 16]. A wide array of pharmacological properties associated with 1-(acyl/aryl)-3-(substituted)thioureas has made them attractive templates for future drug design.

In recent years, there has been a pronounced drive to investigate the topology and conformational aspects of these thioureas prior to their use in various applied fields [17, 18]. A strong prevalence of intramolecular hydrogen bonding [19] largely dictates their aptitude towards complexation [20], cyclization reactions [21], anion recognition [22–24], and drug design [25, 26]. More recently, we have reported [27] that Hirshfeld surfaces analysis [28–30] is an impressive tool for evaluating intermolecular interactions in a small cluster of 1-(adamantane-1-carbonyl) thioureas.

Koch presented a review article on the coordination behavior of *N*-alkyl- and *N,N*-dialkyl-*N'*-acyl (aryl) thioureas with platinum group metals [31], while Aly et al. documented an updated survey of aryl-substituted thioureas and their applications [32]. In 2014, we published a comprehensive report to highlight the promising features of 1-(acyl/aryl)-3-(substituted)thioureas [4]. In view of above-mentioned highlights, there is a quest to explore advances associated with them. In this article, we mainly discuss heterocyclization reactions, topology and corresponding structural aspects, applications, and biological activities of title compounds. We anticipated that this work will be of great interest for researchers concerned with the scope of this demanding framework.



Scheme 1 General chemical structure of 1-(acyl/aryl)-3-(substituted)thiourea

Synthesis

Although various other methods for synthesis of acyl thioureas are available [4], the most important and still an attractive and practical route to access 1-(acyl/aroyle)-3-(substituted) thiourea is Douglas Dains' method [33]. This protocol involves the reaction of in situ generated acyl isothiocyanates from corresponding acid chloride and potassium or ammonium thiocyanate [34], with a suitably substituted aliphatic or aromatic amine usually in dry acetone or acetonitrile (Scheme 2).

Heterocyclization reactions

In this section, recent progress on heterocyclization reactions involving the acyl thiourea group are presented. Wang et al. carried out an operational palladium(II)-catalyzed intramolecular cyclization of substituted 1-acetyl-3-(2-phenyl)thioureas through C(sp²)-H functionalization/CS bond formation (see Scheme 3). Diversity-oriented *N*-benzothiazol-2-yl-amides were obtained efficiently in very good yields. Benzoylthiourea precursors can be synthesized in a cost-effective manner, beginning from inexpensive aryl acid chloride and aryl amines [35].

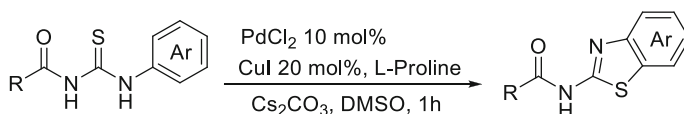
The reaction mechanism can be suggested according to the related palladium-catalyzed processes. The presence of Cs₂CO₃ converts the acetyl-3-(phenyl)thiourea to the thioenolate ion then pre-association of the S atom in the thioenolate to palladium acetate Pd(OAc)₂ promotes the ortho-palladation process followed by release of chloride ions. The synthesis of the 6-membered palladacycle and the successive reductive elimination leads to the formation of *N*-benzothiazol-2-yl-amide and palladium (0). The resulting Pd (0) species are finally reoxidized to Pd (II) by copper iodide (CuI), hence completing this catalytic cycle as shown in Scheme 4.

We reported the cyclization of sulfanilamide thioureas as practical templates for the preparation of iminothiazoline-sulfonamide hybrids with propargyl bromide in the presence of DBU (1,8-Diazabicyclo[5.4.0]undec-7-ene) as a non-nucleophilic base (see Scheme 5). All the resultant iminothiazoline-sulfonamide fusions were tested against Jack bean urease inhibition activity and found to be more effective than standard thiourea [36].

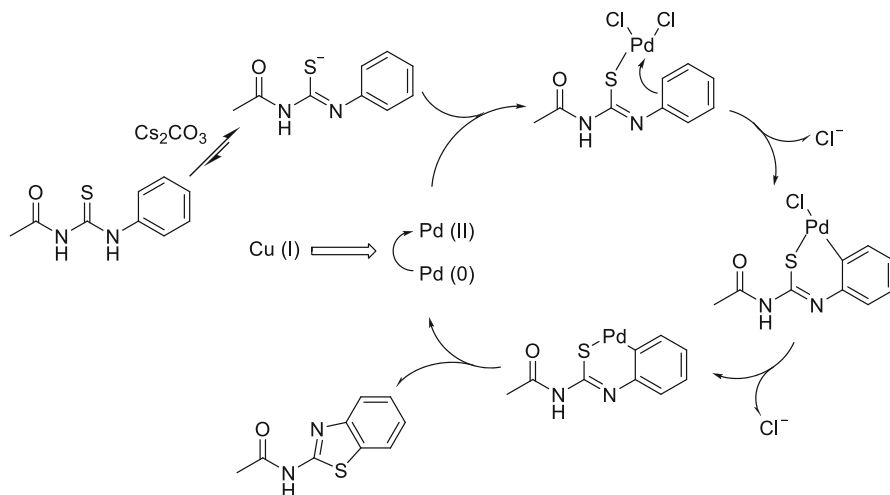
Odame and coworkers reported a regioselective perspective of acyl thioureas heterocyclization to benzimidazole and carried out computational studies to infer the reactivity of selected amino acid-derived benzoyl isothiocyanate incorporating an acyl thiourea backbone. A small library of compounds **1-4** was afforded by the reaction of benzoyl isothiocyanate with L-serine, L-proline, D-methionine and L-alanine. *o*-phenylene diamine moiety attacked exclusively at the carbonyl group



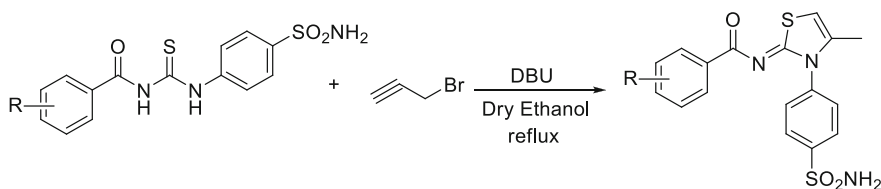
Scheme 2 Synthesis of 1-(acyl/aroyle)-3-(substituted)thiourea



Scheme 3 Pd-catalyzed cyclization of 1-acyl-3-(2-phenyl)-thioureas



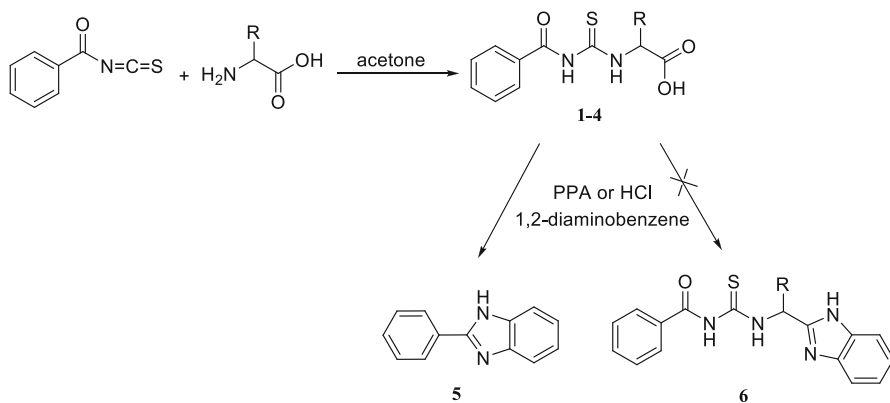
Scheme 4 Suggested reaction mechanism for intramolecular cyclization of substituted 1-acyl-3-(2-phenyl)thioureas



Scheme 5 Heterocyclization of sulfanilamide thioureas to iminothiazoline derivatives

next to the aromatic ring of compounds **1–4** to give substrate **5** as the reaction product rather than at the carboxylic acid group, to furnish **6** (Scheme 6).

According to DFT calculations, the small HOMO–LUMO gap of benzoyl isothiocyanate associated with intramolecular charge transfer is responsible for its substantial high reactivity. The study of frontier orbitals exposed that HOMO is concentrated mostly over the sulfur atom of the thiocarbonyl group whereas LUMO is spread over the thiocarbonyl and the whole molecule except for the carboxylic group which thus remains quiet for participation in the reaction pathway. These findings authentically dictate the fate of the reaction that formation of benzimidazoles took place via cyclization on the benzoyl group rather than on the carboxylic acid site. The authors deduced that, owing to the restricted rotation around the



Scheme 6 Benzimidazole formation via cyclization on the benzoyl group

hetero atom of the proline ring, 1-(benzoyl carbamothioyl)pyrrolidine-2-carboxylic acid **2** undoubtedly exists as rotamers, as evident from the ^{13}C NMR spectrum indicative of the six methylene groups [37].

Recently Aly et al. revealed the reaction pathway to 1,2,4-oxathiazoles employing the 1,1,2,2-ethenetetracarbonitrile (TCNE) reagent to heterocyclize aryl thiourea precursors in dioxane (Scheme 7). Biological and antioxidant activities of newly synthesized heterocyclic cores were screened and SAR studies were inspected [38]. The proposed reaction pathway is shown in Scheme 8.

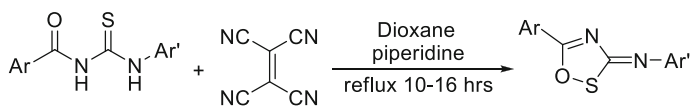
Pape et al. established an efficient protocol introducing a cost-effective and eco-friendly iron trichloride reagent to prepare a cluster of architecturally diverse *N*-benzoylguanidines. This strategy offered FeCl_3 as an alternative to the toxic HgCl_2 metal salt to afford acyl guanidines in good yields by desulfurization of stable *N*-benzoyl thiourea precursors [39] (Scheme 9).

It is concluded that the acyl thiourea motif is an appealing template for the construction of numerous biologically important heterocyclic cores that are embedded in the acyl thiourea architecture.

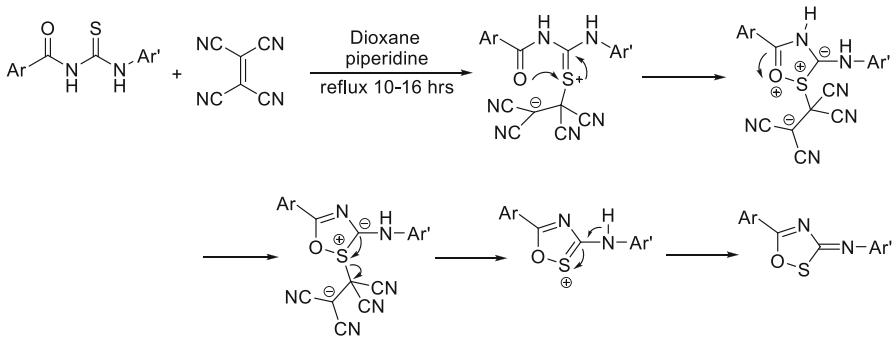
Molecular and crystal structure

Conformational and structural properties

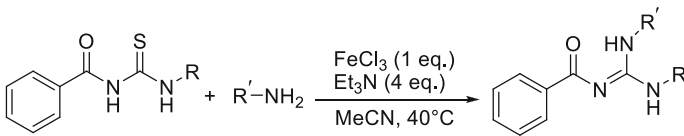
Increasing attention is being committed to the conformational and structural elucidation of 1-(acyl/aryl)-3-(mono-substituted) thiourea derivatives, as these properties are responsible for the behavior of these compounds as ionophores for ion



Scheme 7 Heterocyclization of aryl thioureas with TCNE



Scheme 8 Postulated reaction pathway for 1,2,4-oxathiazoles



Scheme 9 Conversion of *N*-benzoyl thioureas to acyl guanidines

selective electrodes [40–43] and chemosensors for selective and sensitive naked-eye recognition of anions [22–24, 44]. In particular, thiourea fragments and the acceptor anions take part in hydrogen bond interactions [26], and in terms of biological activity these compounds also play an essential role [45].

Saeed and coworkers described two closely related thioureas having 1-(1-naphthoyl) group and 3-(2,4-di-fluoro-phenyl) (**7**) and 3-(3-chloro-4-fluoro-phenyl) (**8**) substitution. The X-ray crystal and molecular structures have been determined resulting in a planar acyl thiourea group, with the C=S and C=O adopting a pseudo-antiperiplanar conformation. A N–H...O=C intramolecular hydrogen bond occurs between the carbonyl and thioamide groups. The crystal packing of both compounds

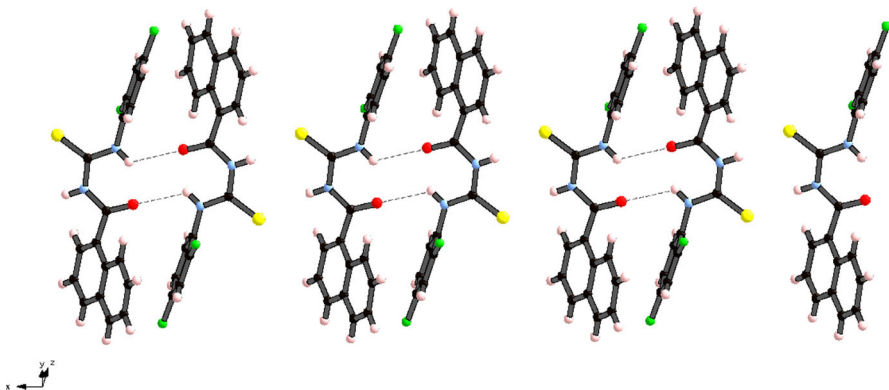
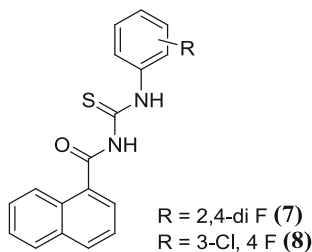


Fig. 1 Partial packing diagram showing the H-bonded chains extending along the *x* direction in the crystal

was characterized by extended intermolecular N–H⋯S=C and N–H⋯O=C hydrogen-bonding interactions involving the acyl thiourea moiety (Fig. 1). π -stacking between adjacent naphthalene and phenyl rings further stabilized the compound (**8**). The vibrational properties, as well as the thermal behavior, studied by Raman and infrared spectroscopy data complemented by quantum chemical calculations supported the formation of these intra- and intermolecular hydrogen bonds. Also, the UV–Vis spectrum was inferred in terms of TD–DFT quantum chemical calculations with the shapes of the simulated absorption spectra in good agreement with the experimental data [46].



A new 1-(2-chlorobenzoyl)thiourea **9** species has been reported by Saeed and coworkers. The X-ray structure analysis validated that an intramolecular N–H⋯O=C hydrogen bond occurs between the thioamide (–NH₂) and carbonyl (–C=O) groups. Moreover, intermolecular interactions in the crystal were characterized by periodic system electron density and topological analysis, and the crystal packing was determined by extended N–H⋯S=C hydrogen-bonding networks between both the carbamide (NH₂) and thioamide (N–H) motifs and the thiocarbonyl bond (C=S) (Fig. 2). The natural bond orbital (NBO) population scrutiny established that strong hyper-conjugative remote interactions are responsible for both inter- and intramolecular interactions. Atom in molecule (AIM) results demonstrated that the N–H⋯Cl intramolecular hydrogen bond between the 2-Cl-phenyl ring and the amide group in the free molecule changed to an H–N⋯Cl interaction as a result of crystal packing [47].

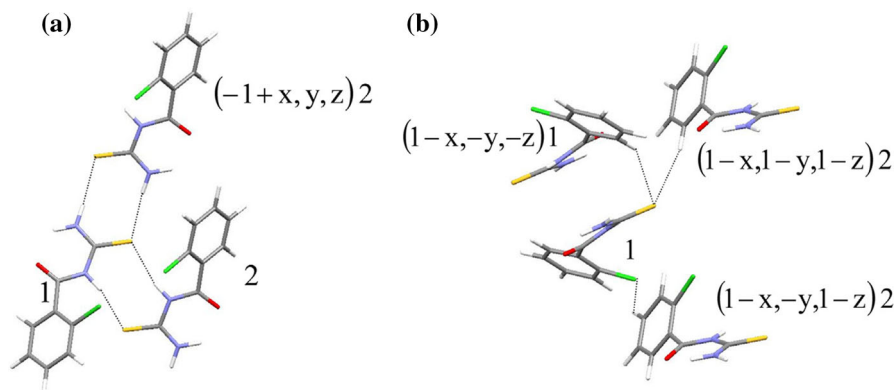
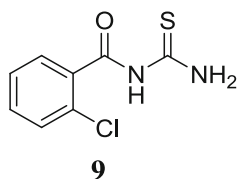
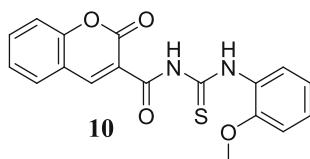


Fig. 2 Main intermolecular interactions in the crystal of 1-(2-chlorobenzoyl)thiourea. **a** N–H⋯S=C building $R_2^2(8)$ motifs. **b** C–Har⋯S and C–Har⋯Cl. The symmetry operation generating the molecule is shown in *parentheses*



The inclusion of more electronegative fluorine atoms in the benzoyl group leads to similar conformational properties and the formation of intra-molecular N–H···F hydrogen bond is further favored [48, 49].

Hirshfeld surface analysis of coumarin-based acyl thiourea **10** was also accomplished by the Saeed research group. Both the coumarin and the phenyl rings were nearly coplanar with the central 1-acylthiourea motif, with the C=S and C=O bonds adopting an opposite orientation. The presence of coumarin and 2-methoxy-phenyl groups attached to the 1-acyl thiourea core supported the formation of an intricate intra- and intermolecular hydrogen bond network and assisted the development of π – π stacking interactions. The crystal packing was stabilized by irregular C–H···O, C–H···S and C–H···C hydrogen bonds, and π – π stacking interactions by offset or slipped facial arrangements (Fig. 3) [50].



Saeed and coworkers published a report to understand the structural features of conformationally congested species 1-(adamantane-1-carbonyl)-3-(2,4,6-trimethylphenyl)thiourea, **11**. A detailed analysis of the intermolecular interactions in a series of six closely associated phenylthiourea derivatives containing the 1-(adamantane-1-carbonyl) group has been reported based on the Hirshfeld surfaces and their related two-dimensional fingerprint plots. The dihedral angle between the 2,4,6-

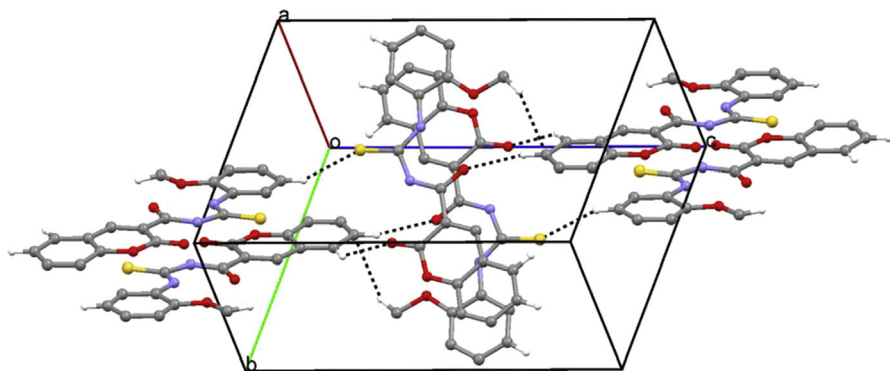
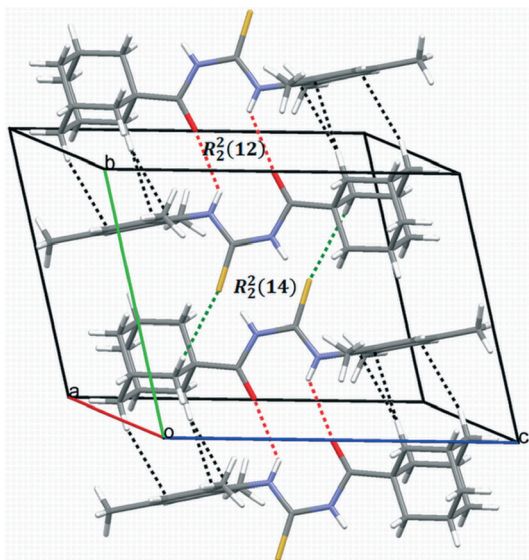
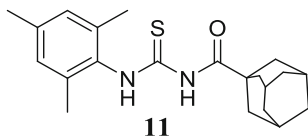


Fig. 3 Crystal packing diagram of 1-(2-oxo-2H-chromene-3-carbonyl)-3-(2-methoxyphenyl)thiourea

Fig. 4 Packing diagram showing centrosymmetric dimers stacked along the *b*-axis. Intra- and inter-molecular hydrogen bonds are shown as dashed lines

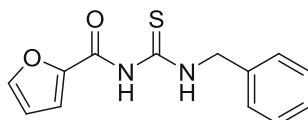


trimethylphenyl motif and the plane of the thiourea fragment is $89.56(5)^\circ$, displaying a twisted conformation (Fig. 4). It is worth noting that the vacuum-isolated molecule exhibited nearly perfect C_s symmetry. According to the enrichment ratios, the H \cdots H contacts were favored, and the S \cdots H contacts have a high tendency to form in the crystals for all the structures. The O \cdots H and C \cdots H links displayed a high tendency to occur in five structures. The presence of the less common C–H \cdots F and C–H \cdots Cl hydrogen bonds, in addition to π – π and C–H– π contacts, was shown to be as important as the conventional interactions in directing the molecule packing. These consequences could be functional in crystal engineering for the design of a supramolecular provision using the 1-(adamantane-1-carbonyl) thiourea synthon [27].

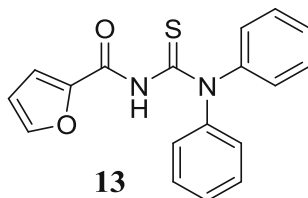


Gil et al. [52] carried out a complete structural, thermodynamic, vibrational and electronic investigation along with UV–visible, FTIR, Raman, NBO analysis and AIM approach for thiourea derivative, 1-benzyl-3-(2-furoyl) thiourea **12**, via the density functional method (B3LYP) with different basis sets. The complete assignment of all vibrational modes was carried out on the basis of the designed frequencies and compared with the reported IR and Raman spectra for that thiourea compound. Time-dependent density functional theory (TD–DFT) was employed to record and analyze the UV–visible absorption spectra. The calculated values for the geometrical parameters of the compound were consistent with the ones reported from XRD studies.

In the crystal structure reported by Pérez et al., compound **12** displayed a tetragonal crystal system and its crystal structure was stabilized by intermolecular interactions such as N–H···S and N–H···O hydrogen bonding [51]. The bond lengths C=O and C=S of the carbonyl and thiocarbonyl groups calculated at the B3LYP/6-311++G(*d,p*) level are 1.227 and 1.678 Å, respectively, and they have a typical double-bond character. However, the C–N bond lengths for the molecule are all shorter than the average single C–N bond length (1.472 Å). The intramolecular hydrogen interaction and ellipticity studied by the AIM approach showed a weak π -character of the bond and hydrogen interactions in the aromatic ring. The stability of the molecule arising from hyperconjugative interaction and charge delocalization has been evaluated by NBO analysis [52].

**12**

With an ambition to know about the ion-recognition properties of 1-furoylthiourea derivatives 3,3-disubstituted, Estévez-Hernández and coworkers investigated the spectroscopic characterization and crystal structure analysis from X-ray powder diffraction data of the 1-Furoyl-3,3-diphenylthiourea (FDFT), **13**. The thiourea group made a dihedral angle of 73.8(6)° with the furoyl group. In the crystal structure, molecules were linked by van der Waals interactions, forming one-dimensional chains along the *a* axis. Non-H-bonding interactions were present in the crystal packing, unlike that observed for related structures (Fig. 5) [53].

**13**

Yamin et al. have studied the molecular structure for a series of 3,3-disubstituted 1-acyl thioureas, clearly showing that the C=O and C=S double bonds are oriented in mutually opposite directions [54–56]. Hamza and coworkers discussed the isomerization effect on the three isomers of *N*-(4-chlorobutanoyl)-*N'*-(*o*-, *m*- and *p*-tolyl)thiourea derivatives, **14a–c**. In order to probe the effect of methyl substitution on spectroscopic and structural properties, DFT and TD–DFT calculations were carried out using five hybrid functionals (B3LYP, B3P86, CAM-B3LYP, M06-2X and PBE0) to predict the UV/Vis spectrum, ¹H and ¹³C NMR chemical shifts, FT-IR vibration modes and X-ray parameters (bonds, bond angles and torsion angles) for the isomers. The results disclosed that the isomerization

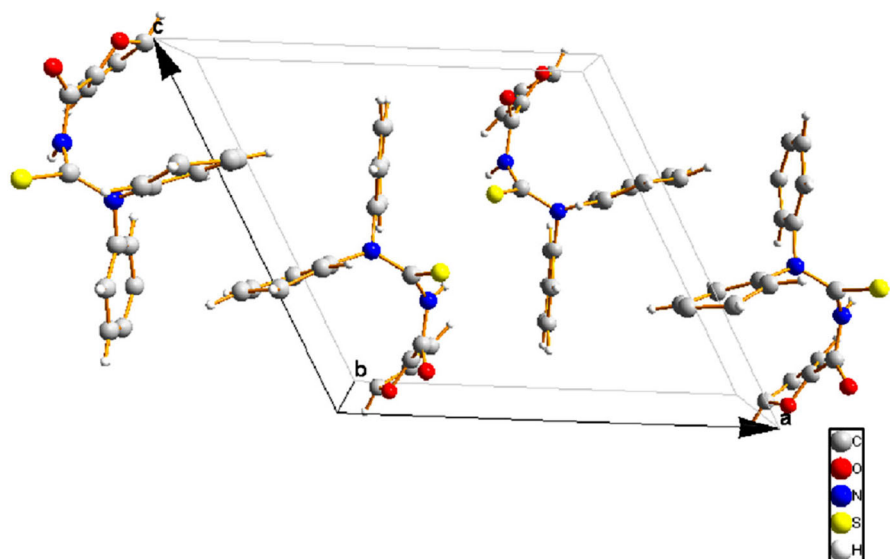
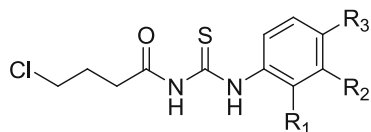


Fig. 5 View of the crystal packing of the FDFT molecules along the *a* axis

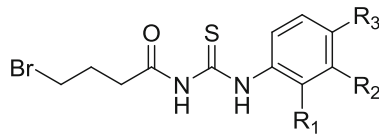
effect was significant on λ_{MAX} absorption bands, while for IR and NMR, the effect was negligible [57].



	R₁	R₂	R₃
14a:	CH ₃	H	H
14b:	H	CH ₃	H
14c:	H	H	CH ₃

In continuation of this work, Hamza and coworkers also illustrated the synthesis, characterization and X-ray structures of *N*-4-(bromobutanoyl)-*N'*-(*o*-, *m*- and *p*-tolyl)thioureas. The two carbonyl thiourea isomers *N*-(4-bromobutanoyl)-*N'*-(3-methylphenyl)thiourea (**15b**) and *N*-(4-bromobutanoyl)-*N'*-(4-methylphenyl)thiourea (**15c**) were obtained in crystalline form by recrystallization employing DMSO as solvent. X-ray crystal analysis revealed that both compounds were crystallized in a triclinic system with space group of *P*-1. The molecules adopted a *trans*-*cis* configuration with respect to the positions of 4-bromobutanoyl and tolyl motifs, respectively, against the thiono C=S bond across their C-N bonds. The configuration was attributed by the intra-hydrogen bond between the carbonyl oxygen and amide hydrogen atoms. Both crystal structures were stabilized by

intermolecular hydrogen bonds $N-H\cdots S$ to form dimers and were arranged along the b axis [58].



	R_1	R_2	R_3
15a:	CH ₃	H	H
15b:	H	CH ₃	H
15c:	H	H	CH ₃

Straightforward synthesis and structural assignment of a new thiourea biphenyl hybrid compound, which is not only a multipurpose ligand for complexation but also an intermediate towards the synthesis of a variety of heterocycles, has been reported by Saeed and Flörke. A few related structures containing the biphenyl thiourea scaffold include *N*-(biphenyl-4-carbonyl)-*N'*-(4-chlorophenyl)thiourea [59], and its 2-chloro, [60], 2-pyridylmethyl [61], and 6-methylpyridin-2-yl [62] analogs, all of these compounds being derived from biphenyl isothiocyanate, whereas Saeed et al. obtained biphenyl thiourea, **16**, from 2,4-dichlorobenzoyl isothiocyanate. The synthesis of the said compound was achieved by reaction of 2,4-dichlorobenzoyl chloride with potassium thiocyanate in a 1:1 molar ratio in dry acetonitrile to give the corresponding isothiocyanate in situ followed by the treatment with 2-aminobiphenyl. The structural assignment was reinforced by spectroscopy, elemental analysis data and crystallographic studies. The compound displayed a monoclinic space group $P2_1/n$ with $a = 13.356(2)$, $b = 7.0761(11)$, $c = 20.539(3)$ Å, $\beta = 105.723(4)^\circ$, $V = 1868.5(5)$ Å³ and $Z = 4$ (Fig. 6) [63].

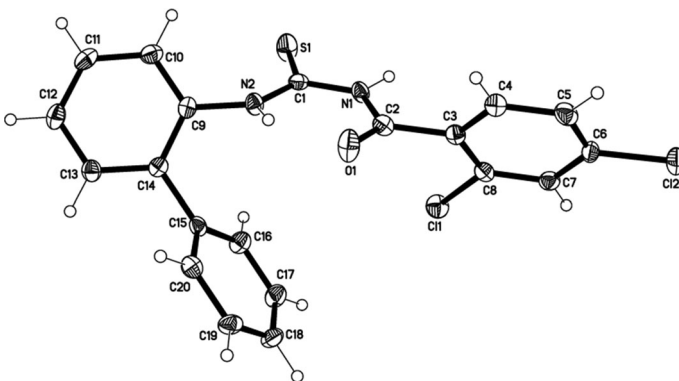
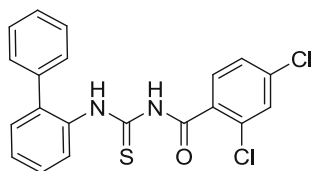
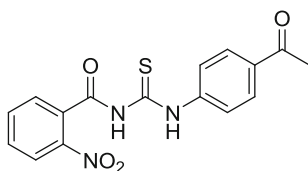


Fig. 6 Molecular structure of the thiourea biphenyl hybrid compound. Anisotropic displacement ellipsoids are drawn at the 50% probability level [63]

**16**

Very recently, Hu and coworkers designed and synthesized *N*-(4-acetylphenyl)-*N'*-(2-nitrobenzoyl)thiourea, **17**. The crystal structure demonstrated the intramolecular hydrogen bonding (N3–H3A···O3 and C10–H10···S1) between the amide-*N* and *o*-nitrobenzoyl-*O* atoms, and the acetylphenyl-C10 and the thiourea-*S*, respectively. Moreover, in the crystals, the compounds were linked to a supramolecular one-dimensional ribbon chain through the intermolecular hydrogen bonds (Fig. 7) [64].

**17**

Metal complexes

Substantial importance has been paid to the synthesis and characterization of acyl/ aroyl thiourea ligands containing the simultaneous presence of *O*, *S*, *N* and *N'* donor atoms and their transition metal complexes, because of their fascinating coordination abilities, structural appearances, and catalytic and biological applications

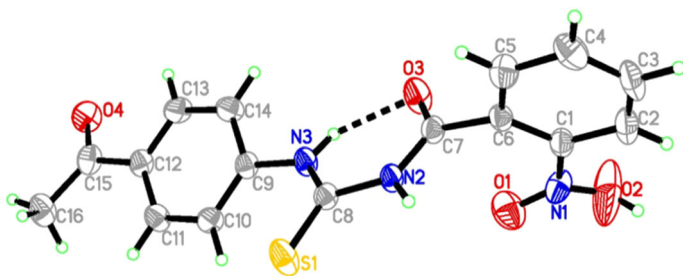
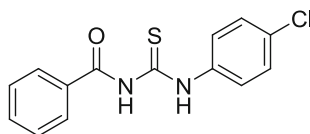


Fig. 7 Molecular and crystal structure of *N*-(4-acetylphenyl)-*N'*-(2-nitrobenzoyl)thiourea [64]

[65–72]. Various thiourea complexes of Pt(II) and Pd(II) have H-bonding and other intermolecular interactions; many of these complexes change their solid state structure in the presence of different counter ions and/or solvents [73–76]. Potential *N*-metal coordination [77, 78] enables some thiourea complexes to cluster via thiourea bridges, yielding an important class of metal cages capable of selectively recognizing (and also detecting) specific anions [79, 80].

Thiourea derivatives possess polar binding sites to build up molecular (self) recognition. Consequently, thiourea metal complexes present inspiring features related to the specific binding modes and to biological properties [81].

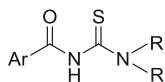
Al-Hazmi et al. prepared metal complexes with 1-benzoyl-3-(4-chlorophenyl)thiourea ligand, **18**. The acyl thiourea derivative contributed as a neutral bidentate towards Pt(IV), Pd(II), and Pt(II) complexes whereas in Co(II) and Ni(II) complexes it acts as a mono-negative bidentate ligand. XRD studies designated the crystalline nature of complexes excluding Cu(II). Homogeneous surface and defined metal ion distribution on the complex surface has been observed for platinum complexes from TEM images. Molecular modeling provided a deep insight into optimized stable structural features [82].



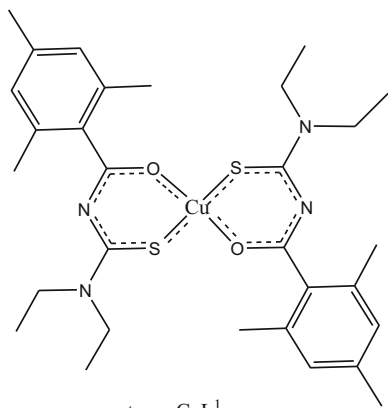
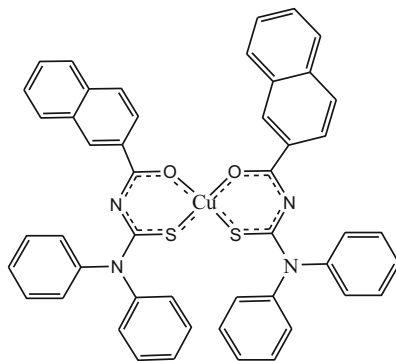
18

On the other hand, when 3,3-di(alkyl)substituted benzoyl thiourea-based ligands form complexes with Ni(II), Cu(II), Fe(III) and Co(II) metals, the anionic O,S chelating coordination mode is preferred [83]. The same coordination is adopted by Pt(II) complexes with 1-(3-chloro)benzoyl-3,3-ethyl thiourea, where a typical square-planar *cis* coordination geometry is formed around the metal [84].

Wu et al. synthesized *N,N*-di-substituted acyl thiourea ligands, **19**, and deprotonated them to form bis-chelate Cu(II) complexes. Single crystal structure analysis revealed that, when the aryl substituent is a bulky 1-naphthalene ring, the resulting Cu(II) complexes were found to exhibit a *cis* arrangement, even modifying the *NRR'* substituents. The structural data proposed that, in order to obtain the *trans* product, Ar and *NRR'* have to be compatible with each other and one of the two must not be more sterically demanding than the other. Taking into account this assumption, the introduction of the mesitylene group offered a subtle size adjustment between naphthalene and substituted Ar rings, as schematized below. By fine-tuning the *NRR'* groups of *N,N*-di-substituted acylthioureas, *trans* Cu(II) complexes were achieved without any fraction of *cis* isomers [85].

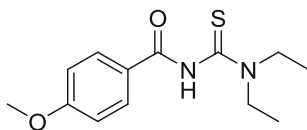


19

*trans*-CuL¹₂L¹ = *N,N*-Diethyl-*N'*-(2,4,6-trimethylbenzoyl)thiourea*cis*-CuL²₂L² = *N,N*-Diphenyl-*N'*-(1-naphthoyl)thiourea

These results demonstrated that, in order to obtain a suitable match and to achieve a small dihedral angle between OCuS planes, the size compatibility of Ar and *NRR'* terminals is very important. It is inferred that, although the *trans* product was exclusively detected, it is still possible that the *cis* isomer could be obtained owing to its thermodynamic stability [86].

Suhud et al. reported the thermodynamics of complexation between Co²⁺ (M) and the 1,1-diethyl-3-(4-methoxybenzoyl)thiourea L, **20**, ligand in various combinations of solvents: (MeCN-DMSO), (MeCN-DCM), (H₂O-DMSO) and (MeCN-H₂O), employing conductometric methods at different temperatures. From these data, it was deduced that the stoichiometry of the neutral complex is 1:3 [M:3L], which suggested that during the course of reaction Co²⁺ oxidized to Co³⁺. The maximum value of stability constant, log₁₀ K_f = 3.31 for the [CoL₃] complex, was observed for the MeCN-DCM (20:80%) binary solvent system at 298.15 K. Thermodynamic parameters for the [CoL₃] complex formation showed that, in most mixed solvent systems, the [CoL₃] complexes were entropy stabilized while enthalpy has a destabilizing effect [87].



20

1-Benzoyl-3-(trimethyl)phenyl thiourea acts as a sulfur-monodentate ligand (κS) toward Rh(I) when [Rh(η^4 -1,5-cyclooctadiene)Cl]₂ is used as precursor [88]. A new series of arene ruthenium [(η^6 -arene)Ru(N \cap S)Cl]PF₆ and Cp*Ir

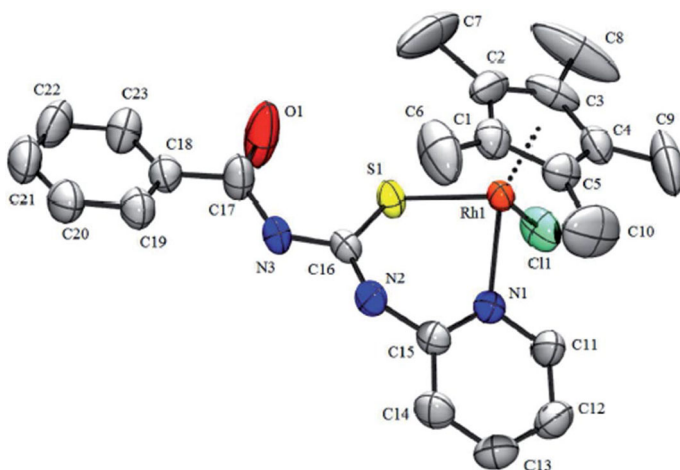


Fig. 8 ORTEP diagram of complex $[Cp^*RhCl(L1)]Cl$ with 50% probability thermal *ellipsoids*. Ref [89]

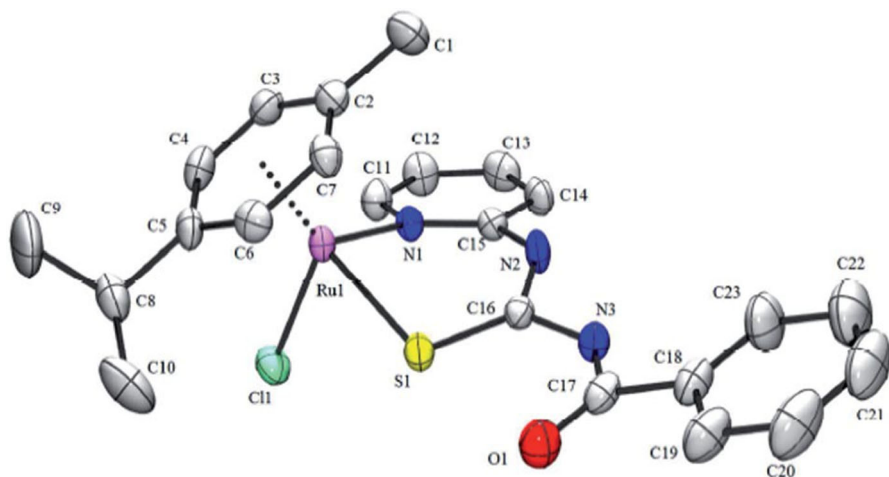
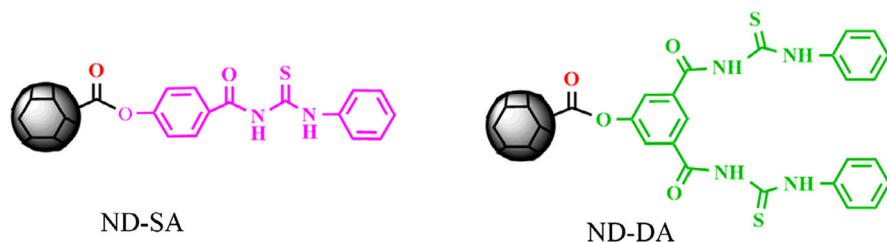


Fig. 9 ORTEP diagram of complex $[(\eta^6\text{-}p\text{-cymene})RuCl(L1)]Cl$ with 50% probability thermal *ellipsoids*. Ref. [89]

Applications

New materials

Uranium, being chief component of nuclear fuel and also an environmentally noxious ingredient, has attracted plentiful attention of many research groups, devoting their efforts for effective separation of uranium from uranium-containing wastes, and there is a pronounced desire to develop solid-phase extraction adsorbents for operative separation of uranyl ions. Merdivan and Zhao established



Scheme 11 Schematic illustration for ND-SA and ND-DA

that uranium can be selectively separated through SPE adsorbents with benzoylthiourea derivatives as functional ligands by the contact between N-CS-NH-CO-Ph chelator and uranyl ions [92, 93].

As triggered by the previous work, the Zhao group carried out for the first time a comparative study to understand the relationship between spatial configurations of the attached functional ligand and the adsorption capacity of the extractant. They developed two unique extractants, ND-SA and ND-DA (Scheme 11), by nanodiamond (ND) modification (single-armed ligand, SA and double-armed ligand, DA) using identical coordination entities acyl thioureas as well-designed ligands [94].

Mechanistic studies suggest a rationale for the action of ND-DA, that it has a tendency to employ its tweezer-like double arms to “lock” metal ions, and the robust chelating power could be inferred from its lower uranium selectivity. In contrast, the agile spatial configuration and judicious complexing capability of ND-SA surprisingly showed superior adsorption selectivity for uranium [94]. This work definitely provides a future orientation for the use of benzoyl thioureas as practical ligands in launching new SPE adsorbents.

The recent era has seen a considerable interest in metal sulfide materials that have found applications in electronics. Taking into account the requirement for innovative semiconducting nanostructured materials for photovoltaics, Saeed et al. [95] designed nickel(II) complexes of various *N*-(dialkylcarbamothioyl)-nitro substituted benzamides, **21a–d**, for the deposition of nickel sulfide semiconducting nanostructured thin films. Golden-colored complexes were stable to air and non-hygroscopic, **21d** was sparingly soluble in THF and acetonitrile and therefore inconvenient for AA-CVD studies. Thin films deposited from precursors **21a** and **21c** exhibited a hexagonal NiS phase, as revealed by the corresponding XRD patterns, while those deposited from complex **21b** showed two dominant phases designated as hexagonal and rhombohedral. AFM determined the extent of surface roughness of the films, as shown in Fig. 10. The SEM and EDX analysis showed a fine dispersion of nickel sulfide in the films, making them possibly expedient semiconducting materials for optoelectronics [95].

Saeed and his group deposited irregular-shaped nickel sulfide nanoparticles from single source precursors Ni complexes by just varying the thioureas ligands [96]. Similarly, trigonal copper sulfide nanoparticles were obtained by thermolysis of Cu(II) complexes having 1-(substituted)benzoyl-3,3-dibutyl thioureas in the presence of oleyl amine as surfactant [97].

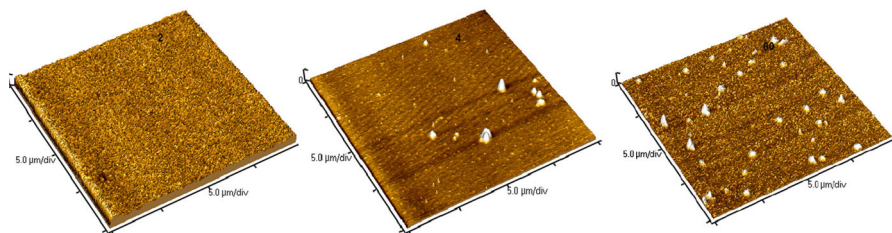
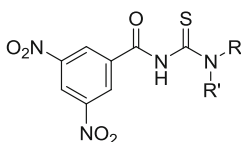
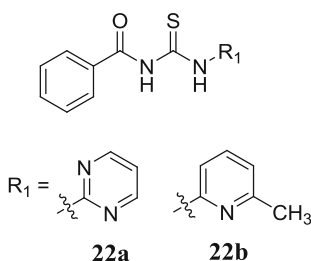


Fig. 10 3D view of AFM images of nickel sulfide thin films deposited from precursors **21a–c** at 723 K [95]



21a = dipropyl; **21b** = hexyl, methyl; **21c** = butyl, ethyl; **21d** = isopropyl, ethyl

Nowadays, the trend of using chemical inhibitors in the chemical process industry for retarding corrosion is being substantially increased and a tremendous pursuit for the usage of thiourea derivatives as anti-corrosion agents for many metals and alloys has been witnessed. Oliveira and coworkers synthesized thiourea derivatives **22a**, and **22b** prior to evaluating their potential for corrosion inhibition with carbon steel in acidic media. Compound **22b** containing a pyridine ring offered superior inhibitory potential near 100% at elevated concentration than the analog featuring a pyrimidine core. The phenomenon of corrosion inhibition involved the adsorption of organic inhibitors on the metal surface as indicated by Langmuir isotherms [98].



The novel compound 1-butyl-3-dodecanoyl thiourea is a non-ionic surfactant that efficiently inhibits the corrosion of chromium and aluminum [99].

Razak et al. reported new 1-(4-substituted)benzoyl thioureas with 3-morpholino-propyl groups with potential liquid crystal properties, as deduced from the study of the molecular structure and vibrational properties [100]. Conductive thin films were fabricated by co-depositing the natural photosensitizer curcumin (extracted from *Curcuma longa*) on an ITO substrate with a new 1-acyl thiourea compound, namely *N*-(octyloxy)phenyl-*N'*-(cinnamoyl) thiourea and *N*-(5-methylpyridine)-*N'*-(1-

naphthoyl) thiourea. The devices exhibited increased conductivity under illumination conditions, with promising applications in organic light-emitting diodes [101, 102]. 1-Benzoyl-3-(3-amino-phenyl) thiourea was immobilized on modified Amberlite-type resin, and the metal uptake capacity evaluated in aqueous solution at pH = 6.0 showing maximum absorption capacity for Cu(II) [103].

As chemosensors

Undoubtedly, the credit goes to the structural framework of acyl thioureas that provide multiple binding sites for chelation of various metal cations and make them a feasible choice for researchers to be used as prominent receptors in the future. Satheshkumar et al. [104] reported a receptor featuring benzoyl thiourea attached to the anthraquinone ring with binding sites fixed in close vicinity for the colorimetric detection of F^- ion. Likewise, the Chauhan group developed phenazine-based thiourea anion sensors [105].

Recently, Suganya and Velmathi developed a small cluster of heterocyclic ring-coupled thiourea anchored on an anthraquinone or phenazine core which acting as signaling moieties for the sensitive and effective recognition of CN^- ion in 25% aq. DMSO in the presence of other co-existing anions. The rapid colorimetric response detected by the color change from orange to purple for **R1–R2** and from light yellow to orange for **R3–R4** manifests the presence of CN^- species as shown in Fig. 11. Screening for fluorescence changes revealed, when the solutions were illuminated under UV light (365 nm), glowing that fluctuated from the green fluorescence of **R3/R4** to other range fluorescence of **R3/R4-CN⁻** complex as shown in Fig. 12. It is noteworthy that the significant fluorescence enhancement observed in phenazine-



Fig. 11 Colorimetric changes of **a R1**, **b R2**, **c R3** and **d R4** (25 μ M in 25% aq. DMSO) upon the addition of various anions (1.5 mM in 25% aq. DMSO) [106]

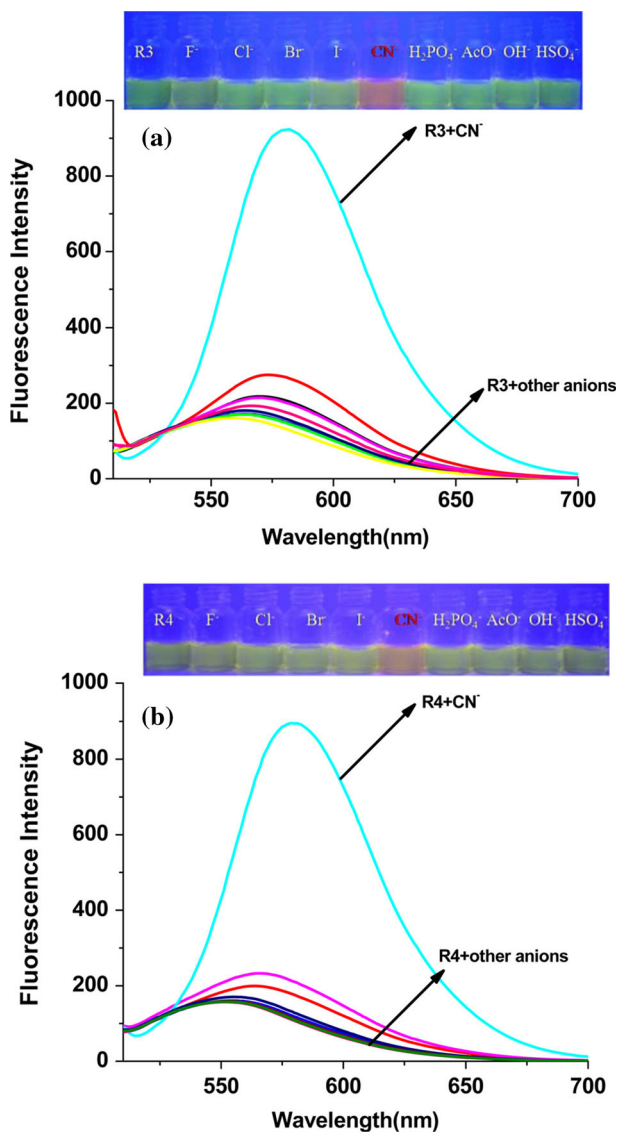
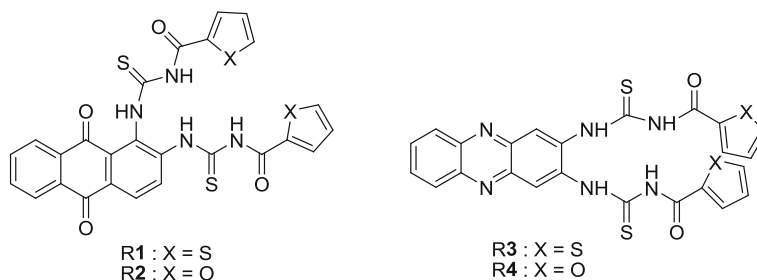


Fig. 12 Fluorescence changes of **a** R3 and **b** R4 (25 μ M in 25% aq. DMSO) upon the addition of various anions (1.5 mM in 25% aq. DMSO). *Inset* color changes under UV light. Ref [106]. (Color figure online)

derived receptors may perhaps be due to improbable participation of the phenazine nucleus during CN⁻ attack and therefore more electron localization within the adduct. The contribution of both the anthraquinone signaling entity and the thiourea binding site in the CN⁻ ion recognizing the route is an allusive rationale for fluorescence quenching in R1 and R2.

The plausible mechanism for the interaction of highly acidic thiourea receptors with cyanide ion involves nucleophilic substitution at carbonyl next to the

heterocyclic rings by the CN^- ion resulting in a cyanohydrin adduct, as is obvious from ^1H NMR titration studies. The β -correction method has been employed to compute the real absorbance of the receptor–anion complex. For practical applications, **R1** and **R2** were used for qualitative assessment of the CN^- ion in cassava flour samples by employing a colorimetric detection technique. Moreover, **R1–R4** were exploited to quantify CN^- ions in tap and drinking water specimens. An outstanding selectivity for CN^- ion and real analytical applications render the current sensors very striking candidates [106].



Different molecular organizations can be found for Hg(II) complexes with 1-acyl thiourea compounds. 1-Benzoyl-3-(substituted)phenyl thiourea complexes of Hg(II) were studied by Okuniewski et al. In general, these complexes displayed distorted tetrahedral geometry around the metal, with intramolecular $\text{N–H}\cdots\text{O}=\text{C}$ hydrogen bonds [107]. Dimeric and polymeric compounds were also obtained by reacting 1-(2-furoyl)-3,3-disubstituted thioureas with HgCl_2 , which are fluorescent materials with their maximum emission at 425 nm [108].

Very recently, Hu and coworkers synthesized yellow crystalline ligand **L 23** and tested its selective chelation capability for the detection of Hg^{2+} in the presence of Ag^+ , Ca^{2+} , Co^{2+} , Ni^{2+} , Cd^{2+} , Pb^{2+} , Zn^{2+} , Cr^{3+} and Mg^{2+} ions [64]. As evident from the reported work, attractive features for a best ion sensor are: (1) only the desired ionic species must induce the pronounced spectral changes, and (2) the recognition of target ion should not be interfered by the simultaneous presence of other competing ions [109, 110]. Ligand **L** emerged as an effective and selective chelator for Hg^{2+} over other coexisting metal cations in DMSO solution (Fig. 13). Desulfurization of thiourea derivative towards Hg^{2+} is the probable recognition route as shown in Scheme 12.

Singh and Rani prepared unique acyl thiourea-tethered organosilatrane and investigated their binding behavior towards heavy and transition metal ions. The receptors exhibited diverse chelation aptitudes for tested Cu^{2+} , Cd^{2+} , Pb^{2+} , and Hg^{2+} ions. Furthermore, the immobilization of pyridine-conjugated bis-thiourea on magnetic silica nano-spheres led to an advanced hybrid nano-material that showed strong adsorption behavior for Cu^{2+} and Pb^{2+} , demonstrating an ability to detect and remove HTM and thus being a new promising nano-receptor [111]. Khairul et al. deposited new thiourea derivatives in polyvinylchloride onto glass substrates by using dip-coating techniques. This thiourea containing an acetylide group which proved to be highly sensitive for the determination of carbon monoxide [112]. The same research team reported the behavior of pyridyl thioureas as ionophores for the

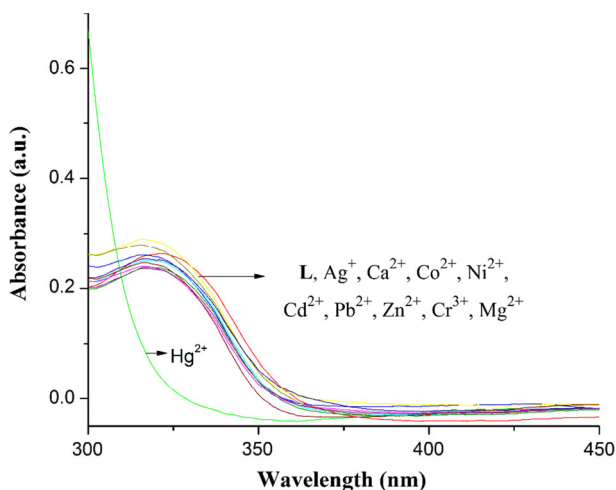
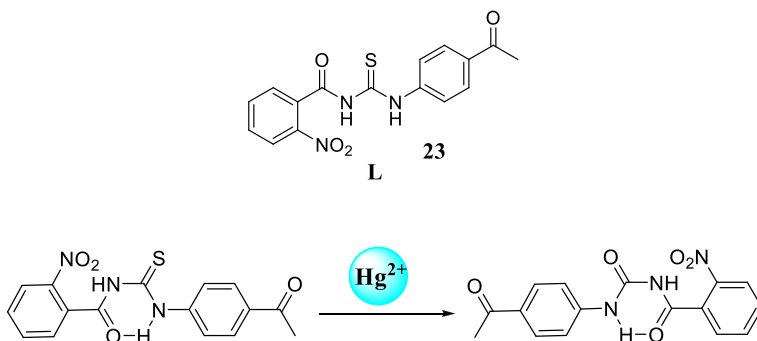


Fig. 13 UV-vis absorption of sensor **L** (2.0×10^{-4} M) in the presence of 20 equiv. various cations in DMSO. Ref [64]



Scheme 12 Possible recognition mechanism

detection of Cu^{2+} . The sensors performed well towards different Cu^{2+} ion concentrations and are being used as striking ionophores [113].

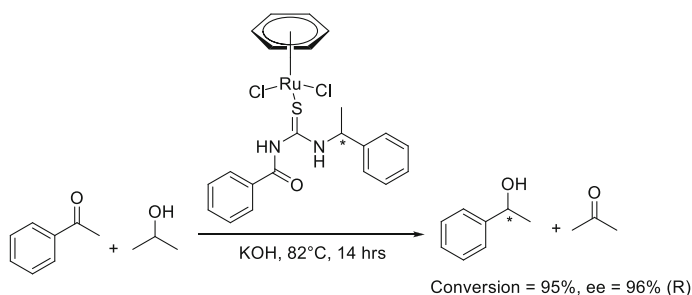
As organocatalysts

The hunt by synthetic chemists for organic catalysts using small organic molecules has entered its fourth decade. It has become one of the most essential types of asymmetric catalysis besides metal and enzyme catalysis. Owing to the ever-increasing need for stereoselective synthesis leading to the desired enantiomer (or diastereomer) as the major or exclusive product, the use of *asymmetric organocatalysis* in drug synthesis (most of which are chiral) is escalating. While cheaper and easily available proline derivatives have successfully been used,

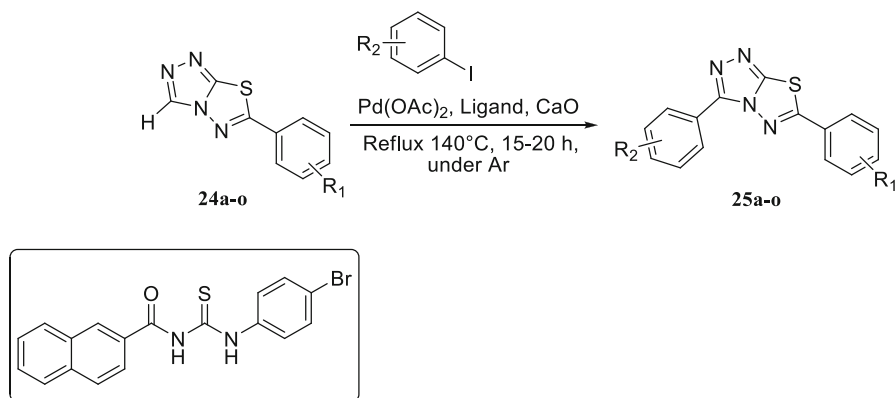
considerable synthetic efforts have been directed towards the design of novel chiral scaffolds for asymmetric organocatalysis. Since 1998, a series of thioureas have been designed, synthesized, and evolved as efficient catalysts for a variety of asymmetric reactions. These belong to the most popular and versatile class of organocatalysts, due to being environmentally friendly and cost-effective, with ease of recovery and reuse and efficacy under mild and neutral conditions, which accommodate acid-sensitive substrates. Furthermore, thiourea catalysts can be bound to polymer resins, are effective in very small amounts and are water-compatible.

A number of reviews are available on the application of thioureas as organocatalysts including that by Gaunt [114] on the use of thioureas in enantioselective organocatalysis, Connon [115] on bifunctional cinchona-based thioureas, Jørgensen on catalytic asymmetric Friedel–Crafts alkylation reactions [116] and Huang [117] on fluorous thiourea organocatalysts. An exhaustive discussion and documentation of all work on thiourea organocatalysis is therefore beyond the scope of this article.

Although a massive literature is available on thiourea-based organocatalysts, as far as the subject of current review is concerned we have only encountered the work of Karvembu et al. [118]. They described half-sandwich Ru(II) complexes $[\text{RuCl}_2(\eta^6\text{-C}_6\text{H}_6)\text{L}]$ with chiral aroyl thiourea ligands having pseudo-octahedral “piano-stool” coordination geometry. The flexibility of these new complexes as catalysts for asymmetric transfer hydrogenation (ATH) of prochiral ketones (including aromatic ketones and hetero aromatic ketones) into resultant optically pure alcohols has been magnificently established, as shown in Scheme 13. High enantioselectivity and outstanding yields reaching up to 99% are the remarkable features of this protocol. ATH reactions proceed via Noyori’s outer sphere mechanism as anticipated by DFT calculations. Another interesting outcome that is worth mentioning is that Ru-benzene complexes proved to be more efficient and attractive for asymmetric reduction of ketones compared to the already reported Ru-*p*-cymene complexes having the same chiral aroyl thiourea ligands [118].



Scheme 13 Transfer hydrogenation of ketones catalyzed by Ru(II) complexes



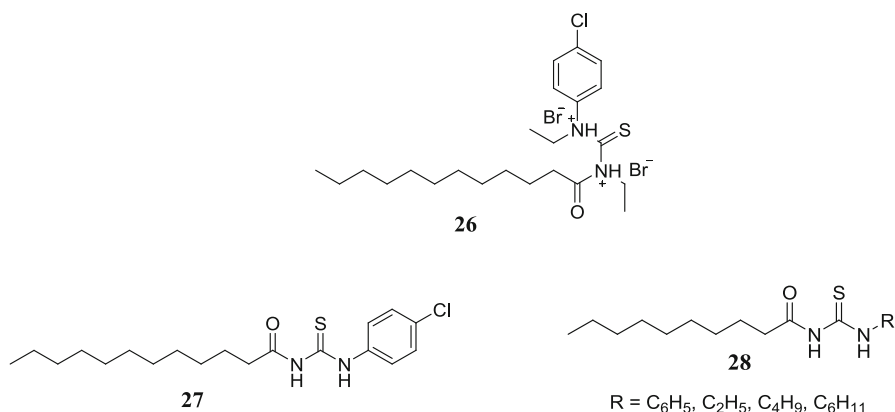
Scheme 14 Coupling of 6-aryl-[1, 2, 4]triazolo[3,4- b][1, 3, 4]thiadiazoles **24a–o** to 3,6-diaryl-[1, 2, 4]triazolo[3,4-b][1, 3, 4]thiadiazoles

By manipulating the approach that thioureas have been exploited as active catalysts for coupling reactions, we recently described the Pd-catalyzed C–H activated cross-coupling of 6-aryl-[1,2,4] triazolo[3,4-b] [1,3,4] thiadiazoles, **24a–o**, with suitably substituted aryl halides by employing 1-(2-naphthoyl)-3-(4-bromophenyl)thiourea as a ligand. The experimental conditions were optimized to afford the target compounds 3,6-diaryl-[1,2,4] triazolo[3,4-b] [1,3,4] thiadiazoles, **25a–o**, in good to excellent yields (Scheme 14) [119].

As surfactants

Surfactants are amphiphilic species and not only limited to cleaning purposes but also enjoying an exciting position in current industrial applications. Acyl thioureas fine-tune the aggregation and adsorption properties of such amphiphiles, making them more striking.

Imdad Ullah et al. reported thiourea featuring cationic surfactant **26** and determined its critical micelle concentration (CMC) using UV–Vis spectroscopy. The surfactants emerged as effective corrosion inhibitors due to the incorporation of thiourea moiety. Low CMC designated them as promising cleaning agents [120]. The same research group documented non-ionic surfactants **27** and **28** containing a thiourea linker in two different reports [121, 122]. Due to sub-millimolar CMCs in the organic solvents and very low water solubility, it was suggested that the surfactants are reasonably amphiphobic. Surfactant **28** exhibited significant antimicrobial potential when tested against a panel of bacterial and fungal strains. It is worth noting that the thiourea moiety not only remarkably contributes towards biodegradable [123, 124] and the eco-friendly nature of these surfactants, but also accounts for their antimicrobial action [125].



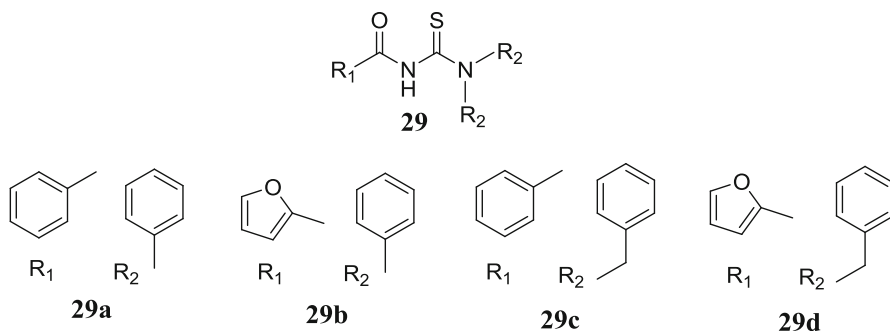
Biological aspects

It is worth noting that much attention has been focused on evaluating the biological potential of 1-(acyl/aryl)-3-(substituted)thiourea derivatives. This has become a fascinating area of research as marked by a plethora of acyl thioureas designed by fine-tuning the structural topographies to obtain fruitful improvements [14, 126, 127]. Here, we throw light on very recently evolved biological approaches to authenticate the efficacy of new stimulating acyl thiourea analogs.

Correa and coworkers studied the interaction of the cis-bis(*N*-benzoyl-*N'*,*N'*-dibenzylthioureido)platinum(II) complex with human (HSA) and bovine (BSA) serum albumin by fluorescence quenching. The protein–Pt complex adduct formation follows a static quenching mechanism and thermodynamic calculations designate one binding site for the interaction of the metal complex with albumin proteins. A Hirshfeld surface study accentuated that non-classical weak C–H⋯C, C–H⋯S and H⋯H intermolecular interactions were essentially responsible for complex-albumin binding. It is noted that acyl thiourea-based Pt complexes have been proved to be potential metallodrug candidates [128].

The same research group extended the work to Ru (II) complexes containing thiourea ligands **29a–d** and evaluated their interaction with BSA and DNA. Fluorescence quenching experiments revealed that the complex interacts with protein via a static quenching mechanism. BSA-binding constants, which were in the range of $3.3\text{--}6.5 \times 10^4 \text{ M}^{-1}$, and the thermodynamic parameters supported moderate and spontaneous interaction of complexes with albumin protein. Low DNA-binding constants ($K_b = 0.8\text{--}1.8 \times 10^4 \text{ M}^{-1}$) and viscosity studies suggested that complexes showed weak binding affinity to DNA. Moreover, Ru(II) complexes were reported to have significantly higher cytotoxic potential than reference drug, cisplatin and free ligands when screened against DU-145 (prostate cancer) and A549 (lung cancer) tumor cell lines [129]. Similarly, a series of half-sandwich Ru(II) (η^6 -p-cymene) complexes bearing aryl thiourea ligands interacted with calf

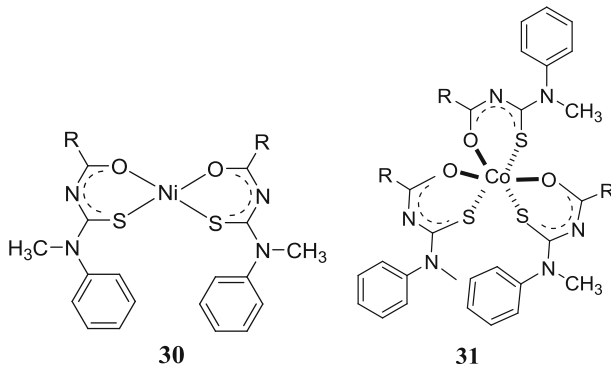
thymus DNA with an intrinsic binding constant in the range of 10^4 M^{-1} in an intercalative mode of binding, cleaving the supercoiled DNA. Cytotoxicity studies showed good activities when the MCF7 ($\text{IC}_{50} = 52.3 \text{ }\mu\text{M}$) and A549 ($\text{IC}_{50} = 54.6 \text{ }\mu\text{M}$) cancer cell lines were analyzed [130].



Zhou et al. demonstrated that Ni(II) complexes of thiourea containing fluorine-benzoyl substituents are efficient antifungal compounds against *Botrytis cinerea*, *Trichoderma* spp., *Myrothecium* and *Verticillium* spp. [131]. Rauf et al. synthesized a cluster of Ni(II) complexes **30** with *N,N,N'*-trisubstituted thiourea ligands and tested for their Jack bean urease inhibitory potential. The compound with no substituent on the phenyl ring ($\text{IC}_{50} = 1.17 \pm 0.12$) was ~ 20 fold more potent than thiourea, and similar superior urease inhibition potency was observed for halo derivatives with IC_{50} of $1.19 \pm 0.41 \text{ }\mu\text{M}$. All the complexes evaluated for in vitro anticancer activity against lung carcinoma (H-157) and kidney fibroblast (BHK-21) cell lines. This study suggested that complexes exhibited significantly more cytotoxic action than *N,N,N'*-trisubstituted thioureas and were perhaps a practical choice for cancer treatment after in vivo and other clinical investigations. Moreover, the complexes displayed notable anti-leishmanial potential in a dose-dependent manner [132].

Later, the same research group evaluated the Co(III) complexes **31** against Jack bean urease and the results undoubtedly indicated that all the complexes failed to show significant inhibition against urease. Cytotoxicity assay revealed that the complexes are promising anticancer agents and non-toxic to normal cells. Among them, analogs with electron-donating groups at the ortho-, meta-, and para-positions of the phenyl ring showed more promising cytotoxic ability than the standard drug, vincristine. The synthesized complexes also exhibited significant inhibitory potential against *L. major* compared to the reference drug, Amphotericin B, and proved to be active anti-leishmanial agents [133].

It is noteworthy that acyl thiourea-based thiophilic metal complexes could be attractive templates for the optimization of future metallo drugs and therapeutic agents. Also, it is obvious that metal ions play a critical role in drug development and efficacy.

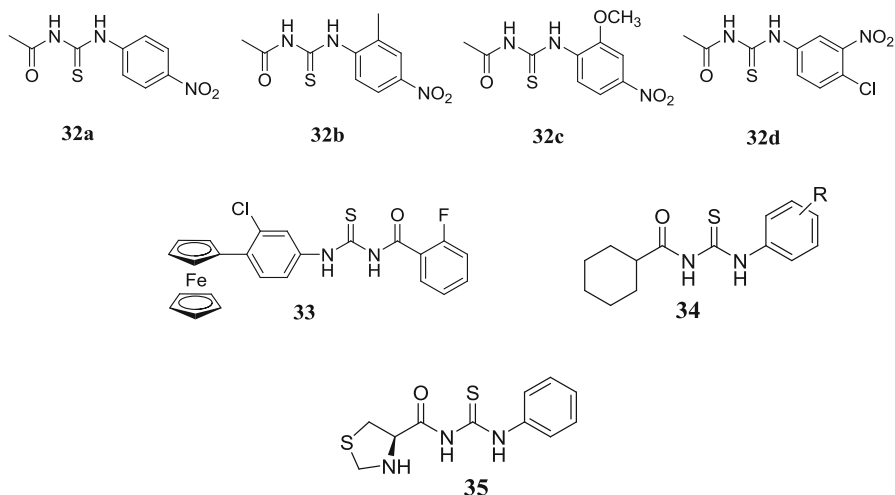


Nitro-substituted acyl thiourea derivatives were synthesized and evaluated for their DNA binding behavior by cyclic voltammetry and UV–Vis spectroscopy. The voltammograms showed a negative shift in peak potential and a bathochromic shift with hypochromism in UV–Vis studies indicate that drug–DNA interaction was found to be electrostatic in nature. The calculated drug–DNA binding constants were in the order of 10^6 M^{-1} . Moreover, the analogs possess moderate antimicrobial potential when screened against a panel of bacterial and fungal strains. Compounds exhibited promising cytotoxic ability with LD_{50} values of 55 ppm for **32a–c** and 60 ppm for **32d**, while DPPH scavenging results exposed their antioxidant potency (see below for the structure of **32a–d**). This study revealed that, among all the four analogs, chloro-substituted thiourea was found to be the most bioactive [134].

Lal et al. investigated the DNA binding potential of 1-(2-fluorobenzoyl)-3-(2-chloro, 4-ferrocenylphenyl)thiourea (2F, **33**) by electrochemical studies. The calculated diffusion coefficient of the 2F–DNA adduct was $8.96 \times 10^8 \text{ cm}^2 \text{ s}^{-1}$ while that of free 2F was $1.75 \times 10^{-7} \text{ cm}^2 \text{ s}^{-1}$ which can be rationalized as free molecules being able to diffuse easily owing to their low molecular weight; however, the compound–DNA adduct becomes heavier and a subsequent decline in current was detected. The ferrocenyl thiourea derivative (2F) also displayed significant antioxidant potential showing IC_{50} of 41.69 $\mu\text{g/ml}$ which indicates that such analogs can be effective clinically [135].

Haribabu and coworkers reported cyclohexyl thioureas **34** ($\text{R}=\text{CH}_3$, H, *p*- OCH_3 , *p*- OC_2H_5 , *o*- CH_3) and screened for anti-oxidant and antihemolytic activities. The synthesized compounds exhibited radical scavenging activity against DPPH assay with IC_{50} of 250 $\mu\text{g mL}^{-1}$ while antihemolytic assay results clearly indicate that compounds are non-toxic. *in silico* molecular docking studies against DprE1 and HSP90 suggested that acyl thioureas may also have antimicrobial and anticancer potentials [136] as DprE1 is an important enzyme for the mycobacterial cell existence and HSP90 is involved in tumor development. Hybrid compounds comprising both thiazolidine and thiourea frameworks, **35**, showed significant

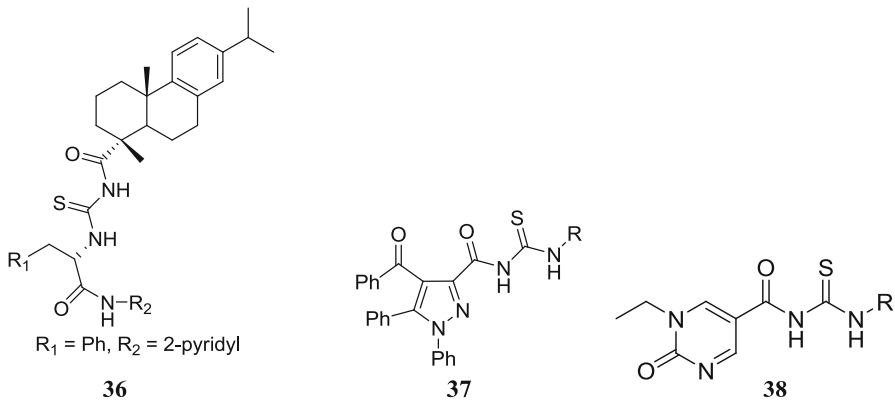
reducing properties and proved to be potent antioxidant candidates in DPPH and ABTS assays [137].



Anticancer activity

Recent published reports have demonstrated that dehydroabiatic acid (DHAA) and their derivatives showed anticancer activity in many human cancer cell lines, including carcinoma cells and breast cancer cells [138]. Following the aim to fine-tune the properties of a pharmacophore and to improve the cytotoxic potential, Jin et al. synthesized DHAA-acyl thiourea-conjugated compounds and screened for in vitro anticancer activity against HeLa, SK-OV-3 and MGC-803 tumor cell lines. Compound **36** presented excellent cytotoxic ability against the HeLa cell line ($IC_{50} = 6.58 \pm 1.11 \mu\text{M}$) and found it superior to the commercial antitumor drug 5-FU ($IC_{50} = 36.58 \pm 1.55 \mu\text{M}$). The incorporation of a phenyl ring at R_1 evidenced increased activity.

The apoptosis-inducing effect of the lead compound was investigated by acridine orange/ethidium bromide staining, Hoechst 33,258 staining, TUNEL assay and flow cytometry which revealed that the compound has a proficiency of apoptosis induction in HeLa cells. The target compound arrested tumor cells in the S phase as depicted by cell cycle analysis. Further studies indicated that a representative DHAA-acyl analog induced apoptosis in cancer cells by a mitochondrial pathway including an increased level of ROS and intracellular Ca^{2+} , the loss of mitochondrial membrane potential and caspase-3 activation [139].



Following the aim to develop a drug that could cause death to cancer cells and stop the further spread of tumours, pyrazole-based thiourea derivatives **37** were tested against human breast and bone cancer cell lines and proved effective and selective Aurora kinase inhibitors. Compounds exhibited better potency than pyrazole itself which may be attributed to their therapeutic efficiency as starting leads for breast cancer medicines [140].

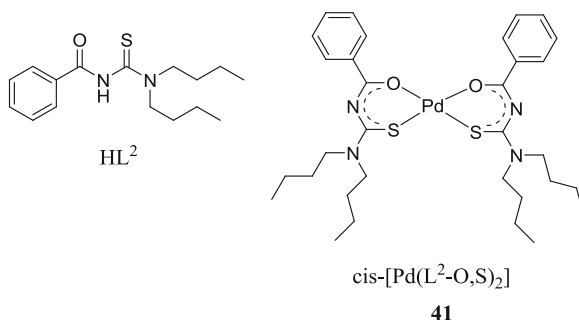
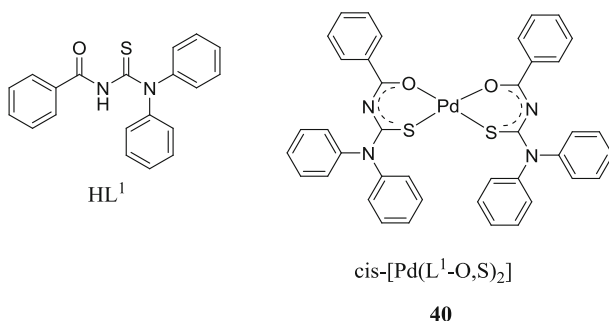
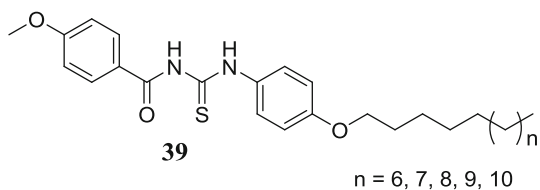
Since Heat Shock Protein 90 (Hsp90) contributes to stabilize and regulate oncogenic client proteins, so developing protein inhibitors is now an emerging and attractive strategy for cancer treatment. Moreover, solubility issues and adverse effects in clinical trials are associated with existing Hsp90 inhibitors. Pyrimidinyl acyl thiourea derivatives **38** were synthesized and evaluated for their cytotoxic action against human invasive ductal breast (MCF-7) and human bone osteosarcoma (Saos-2) cell lines. In vitro and in silico experiments illustrated that the thiourea derivatives were powerful Hsp90 inhibitors, significantly cytotoxic towards both invasive ductal breast carcinoma and bone metastasis, and may prove to be drug template for effective treatment of these malignancies [141].

Anti-amoebic activity

The awareness of possible threats of diseases or infections caused by several types of amoeba is a driving force for evolving anti-amoebic agents. Therefore, the fight against amoebic infections is one of the great successes in the pharmaceutical and medical fields [142]. Khairul et al. published the first report on long-chain alkoxythiourea analogs **39** possessing significant anti-amoebic properties against *Acanthamoeba* sp. The compounds showed considerable potency for growth inhibition of amoeba and damage to their cell membrane permeability as designated by Acridine-orange/Propidium iodide staining. The activity was significantly influenced by the length of the alkyl chain [143].

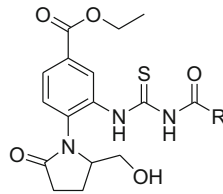
With an ambition to establish transition metal-based active anti-amoebic drug candidates, Maurya et al. synthesized two palladium(II) complexes of *N*-(di(butyl/phenyl)carbamothioyl) benzamide (**40** and **41**) and assayed them for their anti-

amoebic activity against *Entamoeba histolytica*. The in vitro pharmacological screening indicated that both ligands and complexes exhibited outstanding activity profiles with IC_{50} values in the range 0.30–0.80 mM compared to 1.40 for the standard drug, metronidazole. Metal complex $cis-[Pd(L^2-O,S)_2]$ was found to have five times more potency than the reference drug. Further MTT assay-based results demonstrated that all the synthesized compounds showed better cell sustainability and were, hence, less toxic [144].

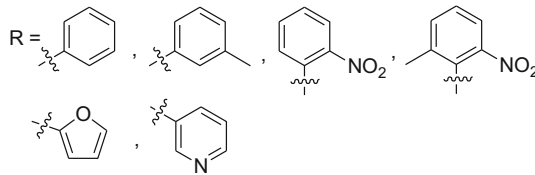


Antiviral activity

Zhou et al. evaluated the antiviral activity of acyl thiourea derivatives **42** against both H1N1 (including its oseltamivir-resistant H275Y strain) and H3N2 influenza A viruses in a cell culture-based assay. The potential of ethyl 4-(2-hydroxymethyl-5-oxopyrrolidin-1-yl)-3-[3-(3-methylbenzoyl)-thioureido] benzoate as an alternative antiviral agent against influenza A viruses was demonstrated [145].



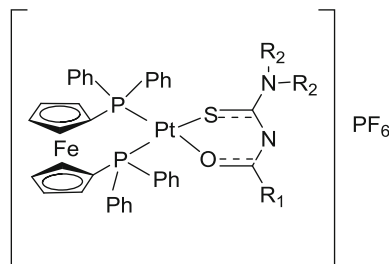
42



Antimicrobial activity

Incorporation of thiourea in pharmaceuticals has become a demanding approach to establish pro-drug templates with enhanced antibacterial properties [146, 147].

Plutín et al. reported novel Pt(II)/dppf/*N,N* disubstituted-*N'*-acyl thiourea complexes **43** and screened them for their antibacterial activity against *M. tuberculosis* H37Rv strains with ethambutol as a standard. The complexes were found to be more potent than free *N,N* disubstituted-*N'*-acyl thiourea ligands that may be ascribed to the significance of the presence of metal ions for superior bioactivity. The nature of R groups has a powerful impact on the activity of complexes as they strongly influence the interaction of metal systems with the *Mycobacterium* membrane [148].

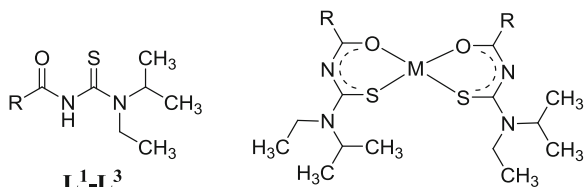


43

Farzanfar and coworkers synthesized three thiourea ligands and their oxido-vanadium(IV) complexes and investigated their antibacterial properties against a panel of bacterial strains. All the analyzed compounds exhibited significant bacterial growth inhibitory potential with MIC values 64–1024 $\mu\text{g mL}^{-1}$. Vanadium(IV)

complexes were more active than non-coordinated thiourea analogs thus emphasizing the importance of metal ions for increase in activity [149].

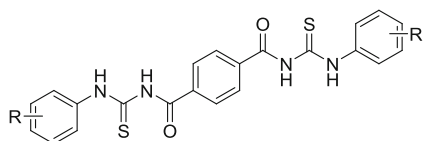
Sumrra et al. synthesized thiourea ligands (L^1-L^3) incorporating thiophenyl and furanyl nuclei ($R =$ thiophenyl, furanyl) and their Co(II), Ni(II), Cu(II) and Zn(II) complexes **44**. The cluster of compounds showed a broad spectrum antimicrobial profile when screened against standard bacterial and fungal strains. Ligands upon coordination with metal ions displayed better bioactivity [150].



$M = \text{Co(II), Ni(II), Cu(II), and Zn(II)}$

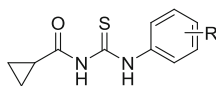
44

1-(phenylene-1,4-dione)-3,3'-(substituted phenyl)-dithiourea **45** and 1-cyclopropanecarbonyl-3-(substituted phenyl)-thioureas **46** were synthesized and tested against different bacterial strains. The compounds showed superior antibacterial activity towards *Salmonella enterica* and *Micrococcus luteus* compared with *Bacillus subtilis* and *Pseudomonas aeruginosa*. Among the series, *m*-hydroxy derivatives were the most potent and a simple reason is that the OH-group is highly polar causing a strong interaction of the compound with the bacterium cell wall [151].



$R = p\text{-Et}; p\text{-OEt}; m\text{-OH}; p\text{-OMe}; \text{naphthyl}$

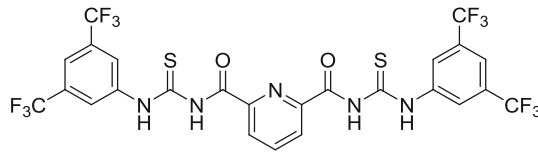
45



$R = p\text{-Me}; p\text{-Et}; p\text{-OEt}; p\text{-Me}; m\text{-OH}; p\text{-OMe}; m\text{-OMe}; 3,4\text{-dimethoxy}; 3,4,5\text{-trimethoxy}; \text{naphthyl}$

46

Nurulain et al. reported bis-thioureas and evaluated them for their antimicrobial activity with streptomycin and kanamycin as positive controls. The compounds failed to exhibit any pronounced activity that may be ascribed to their solubility on the agar surface. However, pyridine-based bis-thiourea **47** showed significant antibacterial activity owing to their enhanced lipophilic character due to trifluoro methyl substituents [152].



47

Currently, researchers are ambitiously engaging in attempts to establish hybrid compounds by connecting privileged frameworks in order to transform their structural features, thus having more promising aspects. So, by exploiting this strategy, Elkholy et al. synthesized thiourea-grafted chitosan derivatives and evaluated their antifungal action against two sugar-beet pathogens, *R. solani* and *S. rolfsii*. All the target compounds possessed significant inhibitory potential against the tested fungal strains. This study verified that chitosan-thiourea derivatives had better antifungal action than simple chitosan [153].

Li et al. demonstrated that chitosan-thiourea derivatives showed excellent bacterial growth inhibition rates compared with natural chitosan when tested against a panel of bacterial strains. The integration of quaternary ammonium and thiourea moieties evidenced improved antibacterial activity due to their enhanced electropositive character. The destructive impact of chemically tuned chitosan derivatives on bacteria was assessed by cell membrane integrity and TEM studies which illustrated that representative compounds damaged bacteria by rupturing the cell membrane [154].

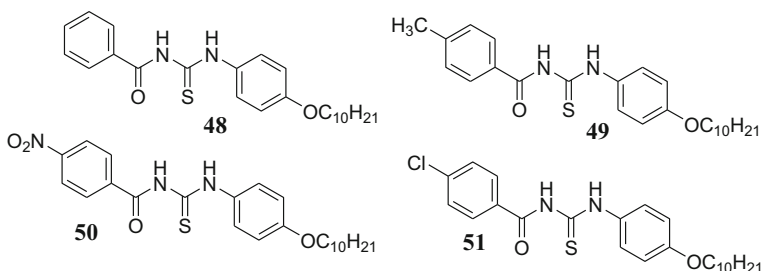
Mohamed et al. prepared pyromellitimide benzoyl thiourea cross-linked chitosan hydrogels and evaluated these super-porous structures for their antimicrobial potential. The hydrogels were found to be more potent towards *Bacillus subtilis* and *Streptococcus pneumoniae* than towards *Escherichia coli*. Antifungal assay results indicated that hydrogels possess efficient antifungal ability against the tested fungal strains. All the chitosan hydrogels showed significantly higher activities than that of the parent chitosan. It is noted that swell ability and antimicrobial potential increase with increased thiourea cross-linker content [155].

Cotelea et al. synthesized a series of 2-phenethylbenzoyl thioureas as potent anti-tubercular agents and estimated their purity and stability profile by employing various physicochemical methods [156].

Anti-algae activity

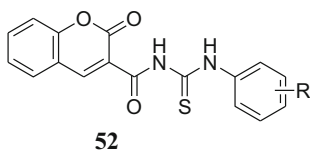
Eutrophication is one of the leading causes of water pollution in aquatic environments. The over-enrichment of nutrients is the potential source of eutrophication which deplete oxygen from water [157, 158] triggering the rapid growth of toxic blue-green algae thus leading to elevated rates of microbial activities [159] and, eventually, to subsequent human health complications. As a new attractive approach to treat the HABs problem, Kasan et al. investigated the practical use of alkoxy thiourea **48–51** derivatives as possible inhibitors towards the growth of toxic blue-green algae *Oscillatoria* sp. in Kenyir Lake, Malaysia. All the

tested alkoxy thiourea analogs exhibited efficient inhibitory effects, compound **49** with methyl substituent being the most potent at a concentration of $18 \mu\text{g mL}^{-1}$ with 37% inhibition [160].



Cholinesterase inhibition activity

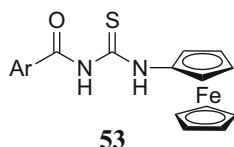
One of the most prevalent neurodegenerative disorders is Alzheimer's disease mainly characterized by memory loss. For an effective treatment of this ailment, acetyl cholinesterase inhibitors play a crucial role. Our research group designed coumarin-based thioureas **52** and evaluated them for their *in vitro* cholinesterase inhibitory potential, with the compound having chloro substituent at the meta position showing the best performance against acetyl cholinesterase ($\text{IC}_{50} = 0.04 \pm 0.01 \mu\text{M}$), whereas the presence of methoxy substituent at the ortho position evinced increased inhibitory activity for butyl cholinesterase ($\text{IC}_{50} = 0.06 \pm 0.02 \mu\text{M}$), while remaining members of the series exhibited significant activity. This study suggested that the rational design of coumarin-based thiourea analogs may prove to be important in advanced drug exploration [161].



Insecticidal and herbicidal activity

Many attempts have been focused on developing new bioactive agrochemicals for crop protection, and acyl thiourea analogs have been documented as attractive templates in this dimension. Recently, benzoyl thioureas featuring a hydantoin skeleton were introduced as potent insecticidal agents [162]. Chengxia and coworkers tested a series of 1-methylcyclohexyl-formyl thioureas and the results revealed that most of the compounds exhibited good herbicidal activities at a concentration of 200 mg/L [163]. In a recent report, the Zhang group identified ferrocenyl thioureas **53** as effective plant growth regulators. Most compounds displayed promising auxin and cytokinin activities and also for their application as plant hormones [164]. *N*-(4-acetylphenyl)-*N'*-(2-nitrobenzoyl)-thiourea was reported to be a considerable plant-growth regulator by Hu et al. [64]. Brito and

coworkers published the design, syntheses and evaluation of benzoyl thioureas as potential urease inhibitors of agricultural importance [165].



Conclusions and future goals

The above discussion has certainly revealed that the easily accessible 1-(acyl/aroil)-3-(substituted) thiourea moiety is a multipurpose, flexible and powerful tool in the hands of organic chemists to manipulate it in various dimensions. This versatile reagent offers quick routes to various diversity-oriented heterocycles and acyl guanidines. The structural and conformational features of 1-(acyl/aroil)-3-(substituted) thioureas, their ligand properties, coordination behavior towards transition metals, and the effect of substituents dictating the configuration and stability of resultant metal complexes have been discussed. Their use as chemosensors for ion recognition, as metal extractors, and as organic single source precursors for the deposition of metal sulfide nano-particles have also been emphasized. As far as the biological potential of 1-(acyl/aroil)-3-(substituted) thioureas is concerned, we came across many documented examples demonstrating them as an exciting class of lead compounds for drug design by exploiting their drug-like properties. Metal complexes have been shown to possess superior potency compared with ligands thus underlining the role of metal ions in the increment of bioactivity.

This review is an attempt to capture the fascinating aspects of 1-(acyl/aroil)-3-(substituted) thioureas and to open a new window to the researchers that this promising thio framework has plenty of room for further advancements, and we hope that upcoming developments may give further encouraging results with more versatile analogs of rational design with potential applications in organic, materials as well as medicinal chemistry.

Acknowledgements MFE is member of the Carrera del Investigador of the Consejo Nacional de Investigaciones Científicas y Técnicas CONICET (República Argentina). The Argentine author thanks the (CONICET), the ANPCYT (PICT-2130), and the Facultad de Ciencias Exactas, Universidad Nacional de La Plata for financial support.

References

1. A. Saeed, M.F. Erben, M. Bolte, *J. Mol. Struct.* **985**, 57–62 (2011)
2. M. Atiş, F. Karipcin, B. Sarıboğa, M. Taş, H. Çelik, *Spectrochim. Acta Mol. Biomol. Spectrosc.* **98**, 290–301 (2012)
3. N.B. Arslan, C. Kazak, F. Aydın, *Spectrochim. Acta Mol. Biomol. Spectrosc.* **89**, 30–38 (2012)
4. A. Saeed, U. Flörke, M.F. Erben, *J. Sulfur Chem.* **35**, 318–355 (2014)
5. J. Malecki, J. Nycz, *Polyhedron* **55**, 49–56 (2013)
6. F.Z. ElAamrani, J. García-Raurich, A. Sastre, L. Beyer, A. Florido, *Anal. Chim. Acta* **402**, 129–135 (1999)
7. X.-P. Rao, Y. Wu, Z.-Q. Song, S.-B. Shang, Z.-D. Wang, *Med. Chem. Res.* **20**, 333–338 (2011)

8. J.R. Burgeson, A.L. Moore, J.K. Boutilier, N.R. Cerruti, D.N. Gharaibeh, C.E. Lovejoy, S.M. Amberg, D.E. Hruby, S.R. Tyavanagimatt, R.D. Allen, *Bioorg. Med. Chem. Lett.* **22**, 4263–4272 (2012)
9. Z. Zhong, R. Xing, S. Liu, L. Wang, S. Cai, P. Li, *Carbohydr. Res.* **343**, 566–570 (2008)
10. C. Limban, A.-V. Missir, I.C. Chirita, M.T. Caproiu, *Rev. Chim. Bucharest.* **61**, 946–950 (2010)
11. J.-F. Zhang, J.-Y. Xu, B.-L. Wang, Y.-X. Li, L.-X. Xiong, Y.-Q. Li, Y. Ma, Z.-M. Li, *J. Agric. Food Chem.* **60**, 7565–7572 (2012)
12. S.-Y. Ke, S.-J. Xue, *Arkivoc* **10**, 63–68 (2006)
13. S.Y. Abbas, M.A.S. El-Sharief, W.M. Basyouni, I.M. Fakhr, E.W. El-Gammal, *Eur. J. Med. Chem.* **64**, 111–120 (2013)
14. S. Saeed, N. Rashid, P.G. Jones, M. Ali, R. Hussain, *Eur. J. Med. Chem.* **45**, 1323–1331 (2010)
15. S.K. Sivan, R. Vangala, V. Manga, *Bioorg. Med. Chem.* **21**, 4591–4599 (2013)
16. K.H. Chikhaliya, M.J. Patel, *J. Enzyme Inhib. Med. Chem.* **24**, 960–966 (2009)
17. A.R. Katritzky, S.R. Tala, N.E. Abo-Dya, K. Gyanda, B.E.-D.M. El-Gendy, Z.K. Abdel-Samii, P.J. Steel, *J. Org. Chem.* **74**, 7165–7167 (2009)
18. E.E. Oruç, S. Rollas, F. Kandemirli, N. Shvets, A.S. Dimoglo, *J. Med. Chem.* **47**, 6760–6767 (2004)
19. K.S. Eccles, R.E. Morrison, A.R. Maguire, S.E. Lawrence, *Cryst. Growth Des.* **14**, 2753–2762 (2014)
20. C.J. Haynes, N. Busschaert, I.L. Kirby, J. Herniman, M.E. Light, N.J. Wells, I. Marques, V. Félix, P.A. Gale, *Org. Biomol. Chem.* **12**, 62–72 (2014)
21. I. Kulakov, O. Nikitina, A. Fisyuk, D. Goncharov, Z. Shul'gau, A. Gulyaev, *Chem. Heterocycl. Compd.* **50**, 670–676 (2014)
22. M. Bonizzoni, L. Fabbrizzi, A. Taglietti, F. Tiengo, *Eur. J. Org. Chem.* **2006**, 3567–3574 (2006)
23. H.-L. Chen, Z.-F. Guo, Z.-L. Lu, *Org. Lett.* **14**, 5070–5073 (2012)
24. S. Li, X. Cao, C. Chen, S. Ke, *Spectrochim. Acta Mol. Biomol. Spectrosc.* **96**, 18–23 (2012)
25. J. Müller, C. Limban, B. Stadelmann, A.V. Missir, I.C. Chirita, M.C. Chifiriuc, G.M. Nitulescu, A. Hemphill, *Parasitol. Int.* **58**, 128–135 (2009)
26. J. Sun, S. Cai, H. Mei, J. Li, N. Yan, Q. Wang, Z. Lin, D. Huo, *Chem. Biol. Drug Des.* **76**, 245–254 (2010)
27. A. Saeed, M. Bolte, M.F. Erben, H. Pérez, *CrystEngComm* **17**, 7551–7563 (2015)
28. S.K. Seth, I. Saha, C. Estarellas, A. Frontera, T. Kar, S. Mukhopadhyay, *Cryst. Growth Des.* **11**, 3250–3265 (2011)
29. S.K. Seth, D. Sarkar, A.D. Jana, T. Kar, *Cryst. Growth Des.* **11**, 4837–4849 (2011)
30. S.K. Seth, *CrystEngComm* **15**, 1772–1781 (2013)
31. K.R. Koch, *Coord. Chem. Rev.* **216**, 473–488 (2001)
32. A.A. Aly, E.K. Ahmed, K.M. El-Mokadem, M.E.-A.F. Hegazy, *J. Sulfur Chem.* **28**, 73–93 (2007)
33. I.B. Douglass, F. Dains, *J. Am. Chem. Soc.* **56**, 719–721 (1934)
34. A.K. Mukerjee, R. Ashare, *Chem. Rev.* **91**, 1–24 (1991)
35. J.-K. Wang, Y.-X. Zong, X.-C. Wang, Y.-L. Hu, G.-R. Yue, *Chin. Chem. Lett.* **26**, 1376–1380 (2015)
36. A. Saeed, S.U. Mahmood, M. Rafiq, Z. Ashraf, F. Jabeen, S.Y. Seo, *Chem. Biol. Drug Des. A/S*. doi: [10.1111/cbdd.12675](https://doi.org/10.1111/cbdd.12675) (2015)
37. F. Odame, E.C. Hosten, R. Betz, K. Lobb, Z.R. Tshentu, *J. Mol. Struct.* **1099**, 38–48 (2015)
38. A.A. Aly, T.E. Malah, E.A. Ishak, A.B. Brown, W.M. Elayat, *J. Heterocyclic Chem.* doi: [10.1002/jhet.2236](https://doi.org/10.1002/jhet.2236) (2016)
39. S. Pape, P. Wessig, H. Brunner, *J. Org. Chem.* **81**, 4701–4712 (2016)
40. A.R.L. Fraga, G.L. Destri, G. Forte, A. Rescifina, F. Punzo, *J. Mol. Struct.* **981**, 86–92 (2010)
41. D. Wilson, M. de los Angeles Arada, S. Alegret, M. del Valle, *J. Hazard. Mater.* **181**, 140–146 (2010)
42. O. Estévez-Hernández, E. Otazo-Sánchez, J.H.-H. De Cisneros, I. Naranjo-Rodríguez, E. Reguera, *Spectrochim. Acta Mol. Biomol. Spectrosc.* **62**, 964–971 (2005)
43. E. Otazo-Sánchez, P. Ortiz-del-Toro, O. Estévez-Hernández, L. Pérez-Marin, I. Goicoechea, A.C. Beltran, J. Villagómez-Ibarra, *Spectrochim. Acta Mol. Biomol. Spectrosc.* **58**, 2281–2290 (2002)
44. M. Boiocchi, L. Del Boca, D.E. Gómez, L. Fabbrizzi, M. Licchelli, E. Monzani, *J. Am. Chem. Soc.* **126**, 16507–16514 (2004)
45. C. Limban, A.-V. Missir, I.C. Chirita, A.F. Neagu, C. Draghici, M.-C. Chifiriuc, *Rev. Chim. Bucharest.* **62**, 168–173 (2011)

46. A. Saeed, S. Ashraf, J.M. White, D.B. Soria, C.A. Franca, M.F. Erben, *Spectrochim. Acta Mol. Biomol. Spectrosc.* **150**, 409–418 (2015)
47. A. Saeed, A. Khurshid, M. Bolte, A.C. Fantoni, M.F. Erben, *Spectrochim. Acta Mol. Biomol. Spectrosc.* **143**, 59–66 (2015)
48. N. Ngah, N.A. Mohamed, B.M. Yamin, H. Mohd Zaki, *Acta Crystallogr. E*, **70**, o705–o705 (2014)
49. S. Firdausiah, A. Salleh Huddin, S.A. Hasbullah, B.M. Yamin, S.F.M. Yusoff, *Acta Crystallogr. E* **70**, o915–o916 (2014)
50. A. Saeed, S. Ashraf, U. Flörke, Z.Y.D. Espinoza, M.F. Erben, H. Pérez, *J. Mol. Struct.* **1111**, 76–83 (2016)
51. H. Pérez, Y. Mascarenhas, O. Estévez-Hernández, S. Santos Jr., J. Duque, *Acta Crystallogr. E* **64**, o695–o695 (2008)
52. D.M. Gil, M.D. Lestard, O. Estévez-Hernández, J. Duque, E. Reguera, *Spectrochim. Acta Mol. Biomol. Spectrosc.* **145**, 553–562 (2015)
53. O. Estévez-Hernández, J. Rodríguez-Hernández, H. Yee-Madeira, J. Duque, *Rev. Mex. Fís.* **61**, 64–68 (2015)
54. B.M. Yamin, S. Sapari, S.A. Hasbullah, *Acta Crystallogr. E* **70**, o33–o33 (2014)
55. N.W. Awang, S.A. Hasbullah, S.F.M. Yusoff, B.M. Yamin, *Acta Crystallogr. E* **70**, o570–o570 (2014)
56. B.M. Yamin, S.M.M. Hizam, S.F.M. Yusoff, S.A. Hasbullah, *Acta Crystallogr. E* **70**, o602–o602 (2014)
57. H.M. Abosadiya, S.A. Hasbullah, B.M. Yamin, *Spectrochim. Acta Mol. Biomol. Spectrosc.* **144**, 115–124 (2015)
58. H.M. Abosadiya, S.A. Hasbullah, B.M. Yamin, *Chin. J. Struct. Chem.* **34**, 379–385 (2015)
59. A.M. Costero, G.M. Rodríguez-Muñiz, P. Gaviña, S. Gil, A. Domenech, *Tetrahedron Lett.* **48**, 6992–6995 (2007)
60. B.M. Yamin, M.A.M. Arif, *Acta Cryst.* **E64**, o104–o104 (2008)
61. M.A.M. Arif, B.M. Yamin, *Acta Cryst.* **E63**, o3594–o3594 (2007)
62. T. Yesilkaynak, G. Binzet, F.M. Emen, U. Flörke, N. Külcü, H. Arslan, *Eur. J. Chem.* **1**, 2–6 (2010)
63. A. Saeed, U. Flörke, *Chin. J. Struct. Chem.* **34**, 853–857 (2015)
64. J.-H. Hu, J.-B. Li, J. Qi, Y. Sun, *Phosphorus. Sulfur. Silicon Relat. Elem.* 00-00 (2015)
65. N. Gunasekaran, R. Karvembu, *Inorg. Chem. Commun.* **13**, 952–955 (2010)
66. N. Selvakumaran, S.W. Ng, E.R. Tiekink, R. Karvembu, *Inorg. Chim. Acta* **376**, 278–284 (2011)
67. N. Gunasekaran, P. Ramesh, M.N.G. Ponnuswamy, R. Karvembu, *Dalton Trans.* **40**, 12519–12526 (2011)
68. N. Gunasekaran, P. Jerome, S.W. Ng, E.R. Tiekink, R. Karvembu, *J. Mol. Catal. A Chem.* **353**, 156–162 (2012)
69. N. Gunasekaran, S. Ng, E. Tiekink, R. Karvembu, *Polyhedron* **34**, 41–45 (2012)
70. N. Selvakumaran, A. Pratheepkumar, S. Ng, E.R. Tiekink, R. Karvembu, *Inorg. Chim. Acta* **404**, 82–87 (2013)
71. N. Selvakumaran, N. Bhuvanesh, A. Endo, R. Karvembu, *Polyhedron* **75**, 95–109 (2014)
72. N. Selvakumaran, N.S. Bhuvanesh, R. Karvembu, *Dalton Trans.* **43**, 16395–16410 (2014)
73. M.G. Fisher, P.A. Gale, M.E. Light, R. Quesada, *CrystEngComm* **10**, 1180–1190 (2008)
74. S. Nadeem, M.K. Rauf, M. Bolte, S. Ahmad, S.A. Tirmizi, M. Asma, A. Hameed, *Transit. Metal Chem.* **35**, 555–561 (2010)
75. P.A. Gale, M.E. Light, R. Quesada, *CrystEngComm* **8**, 178–188 (2006)
76. P.A. Gale, M.E. Light, R. Quesada, *Chem. Commun.* 5864–5866 (2005)
77. P.A. Gale, M.E. Light, R. Quesada, *Polyhedron* **25**, 901–909 (2006)
78. L.B. Kumbhare, U. Singh, B.G. Singh, A. Wadawale, G. Kedarnath, S.S. Zade, K.I. Priyadarsini, V.K. Jain, *Inorg. Chim. Acta* **374**, 69–78 (2011)
79. S.-T. Cheng, E. Doxiadi, R. Vilar, A.J. White, D.J. Williams, *J. Chem. Soc., Dalton Trans.* 2239–2244 (2001)
80. P. Diaz, D.M.P. Mingos, R. Vilar, A.J. White, D.J. Williams, *Inorg. Chim. Acta* **43**, 7597–7604 (2004)
81. U. El-Ayaan, *J. Mol. Struct.* **998**, 11–19 (2011)
82. G.A. Al-Hazmi, A.A. El-Zahhar, K.S. Abou-Melha, F.A. Saad, M.H. Abdel-Rhman, A.M. Khedr, N.M. El-Metwaly, *J. Coord. Chem.* **68**, 993–1009 (2015)
83. H. Mandal, D. Ray, *Inorg. Chim. Acta* **414**, 127–133 (2014)
84. I. Gumus, U. Solmaz, O. Celik, G. Binzet, G.K. Balci, H. Arslan, *Eur. J. Chem.* **6**, 237–241 (2015)

85. W. Hernández, E. Spodine, A. Vega, R. Richter, J. Griebel, R. Kirmse, U. Schröder, L. Beyer, Z. Anorg. Allg. Chem. **630**, 1381–1386 (2004)
86. S.Y. Wu, X.Y. Zhao, H.P. Li, Y. Yang, H.W. Roesky, Z. Anorg. Allg. Chem. **641**, 883–889 (2015)
87. K. Suhud, L.Y. Heng, M. Rezayi, A.A. Al-Abbasi, S.A. Hasbullah, M. Ahmad, M.B. Kassim, J. Solution Chem. **44**, 181–192 (2015)
88. S. Warsink, A. Roodt, J.A. Venter, P. Riekert Kotze, S. Otto, Z. Anorg. Allg. Chem. **228**, 335–336 (2013)
89. M. Kalidasan, R. Nagarajaprakash, S. Forbes, Y. Mozharivskiy, K.M. Rao, Z. Anorg. Allg. Chem. **641**, 715–723 (2015)
90. H.A. Nkabyo, D. Hannekom, J. McKenzie, K.R. Koch, J. Coord. Chem. **67**, 4039–4060 (2014)
91. H.H. Nguyen, A. Takiden, D. Hauenstein, C.T. Pham, C.D. Le, U. Abram, Dalton Trans. **45**, 10771–10779 (2016)
92. M. Merdivan, M.Z. Düz, C. Hamamci, Talanta **55**, 639–645 (2001)
93. Y. Zhao, C. Liu, M. Feng, Z. Chen, S. Li, G. Tian, L. Wang, J. Huang, S. Li, J. Hazard. Mater. **176**, 119–124 (2010)
94. X. Zhao, S. Zhang, C. Bai, B. Li, Y. Li, L. Wang, R. Wen, M. Zhang, L. Ma, S. Li, J. Colloid Interface Sci. **469**, 109–119 (2016)
95. S. Saeed, K.S. Ahmed, N. Rashid, M.A. Malik, P. O'Brien, M. Akhter, R. Hussain, W.-T. Wong, Polyhedron **85**, 267–274 (2015)
96. S. Saeed, N. Rashid, Cogent Chem. **1**, 1030195 (2015)
97. S. Saeed, R. Hussain, J. Coord. Chem. **67**, 2942–2953 (2014)
98. C.G. de Oliveira, V.W. Faria, G.F. de Andrade, E. D'Elia, M.F. Cabral, B.A. Cotrim, G.O. Resende, F.C. de Souza, *Phosphorus. Sulfur. Silicon. Relat. Elem.* **190**, 1366–1377 (2015)
99. I. Ullah, A. Shah, M. Khan, J. Surfactants Deterg. **19**, 873–877 (2016)
100. I.A. Razak, S. Arshad, K. Thanigaimani, M.S.M. Yusof, S.S. Abdullah, A.A. Rahman, Mol. Cryst. Liq. Cryst. **616**, 151–175 (2015)
101. R. Rahamathullah, W.M. Khairul, K. Ku Bulat, Z.M. Hussin, Main Group Chem. **14**, 185–198 (2015)
102. S.M. Jasman, W.M. Khairul, T. Tagg, K. KuBulat, R. Rahamathullah, S. Arshad, I.A. Razak, M.I.M. Tahir, J. Chem. Crystallogr. **45**, 338–349 (2015)
103. A.F. Elhusseiny, A. Eldissouky, A.M. Al-Hamza, H.H. Hassan, J. Mol. Struct. **1100**, 530–545 (2015)
104. A. Satheshkumar, K.P. Elango, Dyes Pigm. **96**, 364–371 (2013)
105. S.M.S. Chauhan, T. Bisht, B. Garg, Tetrahedron Lett. **49**, 6646–6649 (2008)
106. S. Suganya, S. Velmathi, Sens. Actuator B Chem. **221**, 1104–1113 (2015)
107. A. Okuniewski, D. Rosiak, J. Chojnacki, B. Becker, Polyhedron **90**, 47–57 (2015)
108. O. Estévez-Hernández, J. Duque, J. Rodríguez-Hernández, E. Reguera, Polyhedron **97**, 148–156 (2015)
109. C. Chen, R. Wang, L. Guo, N. Fu, H. Dong, Y. Yuan, Org. Lett. **13**, 1162–1165 (2011)
110. S. Malkondu, S. Erdemir, Dyes Pigm. **113**, 763–769 (2015)
111. G. Singh, S. Rani, Eur. J. Inorg. Chem. **2016**, 3000–3011 (2016)
112. A.I. Daud, W.M. Khairul, H.M. Zuki, K. Kubulat, J. Mol. Struct. **1093**, 172–178 (2015)
113. W.M. Khairul, M.F. Hasan, A.I. Daud, H.M. Zuki, K. Kubulat, M.A. Kadir, *MJAS*, **20**, 73–84 (2016)
114. M.J. Gaunt, C.C. Johansson, A. McNally, N.T. Vo, Drug Discov. Today **12**, 8–27 (2007)
115. S.J. Cannon, Chem. Commun. **22**, 2499–2510 (2008)
116. T.B. Poulsen, K.A. Jørgensen, Chem. Rev. **108**, 2903–2915 (2008)
117. Y.-B. Huang, W.-B. Yi, C. Cai, Fluor. Chem. Spring. **308**, 191–212 (2011)
118. M.M. Sheeba, S. Preethi, A. Nijamudheen, M.M. Tamizh, A. Datta, L.J. Farrugia, R. Karvembu, Catal. Sci. Tech. **5**, 4790–4799 (2015)
119. A. Saeed, P.A. Channar, Q. Iqbal, J. Mahar, Chin. Chem. Lett. **27**, 37–40 (2016)
120. I. Ullah, K. Ahmad, A. Shah, A. Badshah, U.A. Rana, I. Shakir, S.Z. Khan, J. Surfactants Deterg. **17**, 501–507 (2014)
121. I. Ullah, A. Shah, M. Khan, K. Akhter, A. Badshah, J. Chem. Sci. **127**, 1361–1367 (2015)
122. I. Ullah, A. Shah, A. Badshah, N.A. Shah, R. Tabor, *Colloids. Surfaces., A.* **464**, 104–109 (2015)
123. L. Yu, *Biodegradable Polymer Blends and Composites from Renewable Resources* (Wiley, London, 2009), pp. 1–465
124. S. Saeed, N. Rashid, A. Tahir, P.G. Jones, Acta Crystallogr. E **65**, o1870–o1871 (2009)

125. T.J. Miles, C. Barfoot, G. Brooks, P. Brown, D. Chen, S. Dabbs, D.T. Davies, D.L. Downie, S. Eyrisch, I. Giordano, *Bioorg. Med. Chem. Lett.* **21**, 7483–7488 (2011)
126. S. Saeed, N. Rashid, P.G. Jones, R. Hussain, M.H. Bhatti, *Cent. Eur. J. Chem.* **8**, 550–558 (2010)
127. S. Saeed, N. Rashid, P. Jones, R. Hussain, *Eur. J. Chem.* **2**, 77–82 (2011)
128. R.S. Correa, K.M. Oliveira, H. Pérez, A.M. Plutín, R. Ramos, R. Mocelo, E.E. Castellano, A.A. Batista, *Arab. J. Chem.* (in press) (2015). doi:[10.1016/j.arabjc.2015.10.006](https://doi.org/10.1016/j.arabjc.2015.10.006)
129. R.S. Correa, K.M. de Oliveira, F.G. Delolo, A. Alvarez, R. Mocelo, A.M. Plutín, M.R. Cominetti, E.E. Castellano, A.A. Batista, *J. Inorg. Biochem.* **150**, 63–71 (2015)
130. K. Jeyalakshmi, J. Haribabu, N.S. Bhuvanesh, R. Karvembu, *Dalton Trans.* **45**, 12518–12531 (2016)
131. C. Li, W. Yang, H. Liu, M. Li, W. Zhou, J. Xie, *Molecules* **18**, 15737–15749 (2013)
132. M.K. Rauf, S. Yaseen, A. Badshah, S. Zaib, R. Arshad, M.N. Tahir, J. Iqbal, *J. Biol. Inorg. Chem.* **20**, 541–554 (2015)
133. S. Yaseen, M.K. Rauf, S. Zaib, A. Badshah, M.N. Tahir, M.I. Ali, M. Shahid, J. Iqbal, *Inorg. Chim. Acta* **443**, 69–77 (2016)
134. S. Tahir, A. Badshah, R.A. Hussain, M.N. Tahir, S. Tabassum, J.A. Patujo, M.K. Rauf, *J. Mol. Struct.* **1099**, 215–225 (2015)
135. B. Lal, S. Akhter, A.A. Altaf, A. Badshah, R.A. Hussain, H. Li, *Int. J. Electrochem. Sci.* **11**, 1632–1639 (2016)
136. J. Haribabu, G.R. Subhashree, S. Saranya, K. Gomathi, R. Karvembu, D. Gayathri, *J. Mol. Struct.* **1094**, 281–291 (2015)
137. T.L. da Silva, L.M.F. Miolo, F.S. Sousa, L.M. Brod, L. Savegnago, P.H. Schneider, *Tetrahedron Lett.* **56**, 6674–6680 (2015)
138. X.-C. Huang, M. Wang, Y.-M. Pan, G.-Y. Yao, H.-S. Wang, X.-Y. Tian, J.-K. Qin, Y. Zhang, *Eur. J. Med. Chem.* **69**, 508–520 (2013)
139. L. Jin, H.-E. Qu, X.-C. Huang, Y.-M. Pan, D. Liang, Z.-F. Chen, H.-S. Wang, Y. Zhang, *Int. J. Mol. Sci.* **16**, 14571–14593 (2015)
140. A. Ozgur, E. Yenidunya, I. Koca, Y. Tutar, *Lett. Drug Des. Discov.* **12**, 180–189 (2015)
141. İ. Koca, A. Özgür, M. Er, M. Gümüüş, K.A. Coşkun, Y. Tutar, *Eur. J. Med. Chem.* **122**, 280–290 (2016)
142. R. Dudley, A. Matin, S. Alsam, J. Sissons, A.H. Maghsood, N.A. Khan, *Acta Trop.* **95**, 100–108 (2005)
143. W.M. Khairul, Y.-P. Goh, A.I. Daud, M. Nakisah, *Arab. J. Chem.* (2015). doi:[10.1016/j.arabjc.2015.05.011](https://doi.org/10.1016/j.arabjc.2015.05.011)
144. M.R. Maurya, B. Uprety, F. Avecilla, S. Tariq, A. Azam, *Eur. J. Med. Chem.* **98**, 54–60 (2015)
145. J. Yu, D. Wang, J. Jin, J. Xu, M. Li, H. Wang, J. Dou, C. Zhou, *Antiviral Res.* **127**, 68–78 (2016)
146. H.M. Faidallah, K.A. Khan, A.M. Asiri, *J. Fluor. Chem.* **132**, 870–877 (2011)
147. A.P. Keche, G.D. Hatnapure, R.H. Tale, A.H. Rodge, S.S. Birajdar, V.M. Kamble, *Bioorg. Med. Chem. Lett.* **22**, 3445–3448 (2012)
148. A.M. Plutín, A. Alvarez, R. Mocelo, R. Ramos, E.E. Castellano, M.M. da Silva, L. Colina-Vegas, F.R. Pavan, A.A. Batista, *Inorg. Chem. Commun.* **63**, 74–80 (2016)
149. J. Farzanfar, K. Ghasemi, A.R. Rezvani, H.S. Delarami, A. Ebrahimi, H. Hosseinpoor, A. Eskandari, H.A. Rudbari, G. Bruno, *J. Inorg. Biochem.* **147**, 54–64 (2015)
150. S.H. Sumrra, M. Hanif, Z.H. Chohan, M.S. Akram, J. Akhtar, S.M. Al-Shehri, *J. Enzyme Inhib. Med. Chem.* **31**, 590–598 (2016)
151. A. Banaei, J.A. Shiran, A. Saadat, F.F. Ardabili, P. McArdle, *J. Mol. Struct.* **1099**, 427–431 (2015)
152. N. Kamalulazmy, S.A. Mutalib, F.I. Nasir, N.I. Hassan, *MJAS* **20**, 5–90 (2016)
153. S.S. Elkholy, H.A. Salem, M. Eweis, M.Z. Elsabee, *Int. J. Biol. Macromolec.* **70**, 199–207 (2014)
154. Z. Li, F. Yang, R. Yang, *Int. J. Biol. Macromolec.* **75**, 378–387 (2015)
155. N.A. Mohamed, N.A.A. El-Ghany, M.M. Fahmy, *Int. J. Biol. Macromolec.* **82**, 589–598 (2016)
156. T. Cotelea, G.M. Nițulescu, P. Oleg, L. Morușciag, *Drugs* **63**, 5 (2015)
157. M.D. Skogen, K. Eilola, J.L. Hansen, H.M. Meier, M.S. Molchanov, V.A. Ryabchenko, *J. Marine Syst.* **132**, 174–184 (2014)
158. K.R. Reddy, R.D. DeLaune, *Biogeochemistry of Wetlands: Science and Applications* (CRC Press, Boca Raton, 2008), pp. 89–119
159. C. Huang, X. Wang, H. Yang, Y. Li, Y. Wang, X. Chen, L. Xu, *Sci. Total Environ.* **485**, 1–11 (2014)

160. N.A. Kasan, S.Z.M. Yusof, N.B. Ramli, W.M. Khairul, H.A. Zakeri, *J. Environ. Sci. Eng.* **4**, 389–394 (2015)
161. A. Saeed, S. Zaib, S. Ashraf, J. Iftikhar, M. Muddassar, K.Y. Zhang, J. Iqbal, *Bioorg. Chem.* **63**, 58–63 (2015)
162. X. Zhihong, L. Bin, D. Hongbo, W. Mingan, *Chin. J. Org. Chem.* **34**, 2517–2522 (2014)
163. Y. Gong, W. Huang, X. Liu, J. Weng, C. Tan, *Chin. J. Org. Chem.* **33**, 2396–2401 (2013)
164. Q. Zhang, B. Zhao, Y. Song, C. Hua, X. Gou, B. Chen, J. Zhao, *Heteroatom Chem.* **26**, 348–354 (2015)
165. T.O. Brito, A.X. Souza, Y.C. Mota, V.S. Morais, L.T. de Souza, Â. de Fátima, F. Macedo, L.V. Modolo, *RSC Adv.* **5**, 44507–44515 (2015)